



**HAL**  
open science

# Dual functional materials capable of integrating adsorption and Fenton-based oxidation processes for highly efficient removal of pharmaceutical contaminants

Muhammad Usman, Olivier Monfort, Sridhar Gowrisankaran, Bassim H Hameed, Khalil Hanna, Mohammed Al-Abri

## ► To cite this version:

Muhammad Usman, Olivier Monfort, Sridhar Gowrisankaran, Bassim H Hameed, Khalil Hanna, et al.. Dual functional materials capable of integrating adsorption and Fenton-based oxidation processes for highly efficient removal of pharmaceutical contaminants. *Journal of Water Process Engineering*, 2023, 52, pp.103566. 10.1016/j.jwpe.2023.103566 . hal-04137888

**HAL Id: hal-04137888**

**<https://hal.science/hal-04137888v1>**

Submitted on 30 Aug 2024

**HAL** is a multi-disciplinary open access archive for the deposit and dissemination of scientific research documents, whether they are published or not. The documents may come from teaching and research institutions in France or abroad, or from public or private research centers.

L'archive ouverte pluridisciplinaire **HAL**, est destinée au dépôt et à la diffusion de documents scientifiques de niveau recherche, publiés ou non, émanant des établissements d'enseignement et de recherche français ou étrangers, des laboratoires publics ou privés.

1 **Dual functional materials capable of integrating adsorption and**  
2 **Fenton-based oxidation processes for highly efficient removal of**  
3 **pharmaceutical contaminants**

4  
5 Muhammad Usman<sup>1,2\*</sup>, Olivier Monfort<sup>3</sup>, Sridhar Gowrisankaran<sup>3</sup>, Bassim H.  
6 Hameed<sup>4</sup>, Khalil Hanna<sup>5</sup>, Mohammed Al-Abri<sup>6,7\*</sup>

7  
8 <sup>1</sup> Center for Environmental Studies and Research, Sultan Qaboos University, Al-Khoud 123,  
9 Muscat, Oman

10 <sup>2</sup> École Nationale Supérieure de Chimie de Rennes, CNRS, UMR 6226, F-35000 Rennes,  
11 France

12 <sup>3</sup> Department of Inorganic Chemistry, Faculty of Natural Sciences, Comenius University  
13 Bratislava, Ilkovicova 6, Mlynska Dolina, 84215 Bratislava, Slovakia

14 <sup>4</sup> Department of Chemical Engineering, College of Engineering, Qatar University, P.O Box:  
15 2713 Doha, Qatar

16 <sup>5</sup> Univ Rennes, École Nationale Supérieure de Chimie de Rennes, CNRS, ISCR-UMR 6226,  
17 F-35000 Rennes, France

18 <sup>6</sup> Nanotechnology Research Center, Sultan Qaboos University, P.O Box 17, Al-Khoud,  
19 Muscat, 123, Oman

20 <sup>7</sup> Department of Petroleum and Chemical Engineering, College of Engineering, Sultan Qaboos  
21 University, P.O Box 33, Al-Khoud, Muscat, 123, Oman

22  
23 **\* For Correspondence:** : [muhammad.usman@squ.edu.om](mailto:muhammad.usman@squ.edu.om) (M. Usman)

24 [alabri@squ.edu.om](mailto:alabri@squ.edu.om) (M. Al-Abri)

25  
26 **ORCID IDs**

27 <http://orcid.org/0000-0001-6900-1333> (M. Usman)

28 <https://orcid.org/0000-0003-2992-8155> (O. Monfort)

29 <https://orcid.org/0000-0001-5171-6189> (B.H. Hameed)

30 <https://orcid.org/0000-0002-5470-8050> (M. Al-Abri)

31 <https://orcid.org/0000-0002-6072-1294> (K. Hanna)

32	<b>Table of Contents</b>	
33	<b>Abstract</b> .....	<b>3</b>
34	<b>1. Introduction</b> .....	<b>4</b>
35	<b>2. Literature Search Methodology</b> .....	<b>7</b>
36	<b>3. Coupling of Heterogeneous Fenton oxidation with adsorption</b> .....	<b>8</b>
37	3.1. Pristine nano zero-valent iron (nZVI) and its composites with other materials.....	<b>8</b>
38	3.2. Pristine iron minerals having dual functions (adsorption and Fenton catalyst) .....	<b>13</b>
39	3.3. Composites of iron minerals and other materials .....	<b>15</b>
40	<b>4. Coupling of photo-Fenton and photocatalysis with adsorption</b> .....	<b>23</b>
41	4.1. Iron-based materials combined with zeolites and porous alumina .....	<b>24</b>
42	4.2. Iron-based materials combined with biomass-based adsorbents.....	<b>25</b>
43	4.3. Iron-based materials combined with g-C <sub>3</sub> N <sub>4</sub> .....	<b>27</b>
44	4.4. Iron-based materials combined with MoS <sub>2</sub> .....	<b>31</b>
45	4.5. Magnetic composites and other sophisticated iron-based materials .....	<b>32</b>
46	4.6. Stability of iron-based materials for integrated adsorption with photochemical process	
47	.....	<b>34</b>
48	<b>5. Conclusions and outlooks</b> .....	<b>34</b>
49	<b>References</b> .....	<b>37</b>
50		
51		

## 52 **Abstract**

53 Pharmaceutical contaminants have shown widespread presence in water/wastewater  
54 threatening environmental and human health. Existing literature shows that adsorption can  
55 efficiently bind pharmaceuticals preventing their transfer into the treated water. However,  
56 adsorption only diverts these contaminants from one phase to another requiring the treatment  
57 of contaminant-laden adsorbents. Fenton oxidation ( $\text{H}_2\text{O}_2$ -based) has shown good potential  
58 for the degradation of pharmaceuticals. But, the practical use of Fenton oxidation is often  
59 limited by its higher chemical demands and low contact of oxidizing species with target  
60 contaminants. Efforts to overcome these practical obstacles aim to develop efficient  
61 heterogeneous catalysts which also benefit from their strong contaminant adsorption capacity.  
62 This is the first review that focuses exclusively on dual-functional materials that can effectively  
63 adsorb pharmaceutical pollutants (separation-based removal) and promote Fenton oxidation  
64 simultaneously (degradation-based removal) in aqueous systems. The dual functionality  
65 enables the integration of adsorption and Fenton-based processes (heterogeneous Fenton,  
66 photo-Fenton and photocatalysis) to efficiently remove pharmaceuticals. This integration can  
67 be achieved using a single material having both functions or by compositing/impregnating  
68 different materials. The properties of these materials have important consequences on their  
69 treatment efficiency, stability, and regeneration ability. These processes and materials are  
70 critically evaluated to illustrate their potential, associated challenges and their key solutions.  
71 Some of these challenges originate from the tested materials while others are inherent to the  
72 treatment process and the prospects for improvement exist at their intersection. Future  
73 research should aim to rationally improve the catalytic and adsorption properties of these  
74 materials and explore their practical implementation in wastewater treatment technologies.

75

76 **Keywords:** Wastewater treatment; Hybrid materials; Advanced oxidation processes;  
77 Adsorption; Emerging environmental pollutants

## 78 **1. Introduction**

79 Pharmaceuticals have been identified as an emerging group of environmental contaminants  
80 due to their potential hazards to human health and ecosystem [1]. Pharmaceutical  
81 contaminants are differentiated from traditional industrial pollutants based on a) their diverse  
82 chemical structures, molecular weight, and functionality, b) they are polar molecules having  
83 more than one ionizable group whereas the degree of ionization is controlled by the solution  
84 pH, c) they are mainly lipophilic in nature though some of them are moderately soluble in  
85 water, d) they have the ability to persist in nature, accumulate in life forms, and remain  
86 biologically active e) after administration, metabolic reactions can modify their chemical  
87 structure [1, 2]. Thus, pharmaceuticals can be excreted without being transformed or  
88 metabolized in the form of more polar and lipophilic derivatives. These properties ultimately  
89 dictate the fate and removal of pharmaceuticals in the environment differently than the  
90 traditional pollutants. Their presence in environment, even in small quantities, can be harmful  
91 because they have been specially designed to exert biological effects even at very low  
92 concentration [3]. Their contamination in aquatic systems is mainly linked to their misuse in  
93 medical and agricultural settings and the release of unregulated effluents (hospital, industrial,  
94 domestic, and agricultural) [4]. For example, according to the US Center for Disease  
95 Prevention and Control, injudicious antibiotic use may approach 50% [5]. This figure could be  
96 worse in developing countries where over-the-counter sales of drugs is highly unregulated [6].  
97 Since traditional water/wastewater treatments are unable to completely eliminate these  
98 compounds [7], finding affordable, efficient, and environmentally benign treatments is highly  
99 desired to maintain ecological security and a clean water supply.

100 Many technologies have been tested to remove pharmaceuticals from aqueous systems.  
101 Among them, adsorption of pharmaceuticals is known for its simplicity, cost-efficiency, quick  
102 pollutant removal, and low sludge production [8, 9]. However, adsorption is a separation-  
103 based technique (a phase changing technology) that simply diverts the pollutants from water  
104 to another phase, yielding contaminant-laden sorbents which require side-stream disposal or

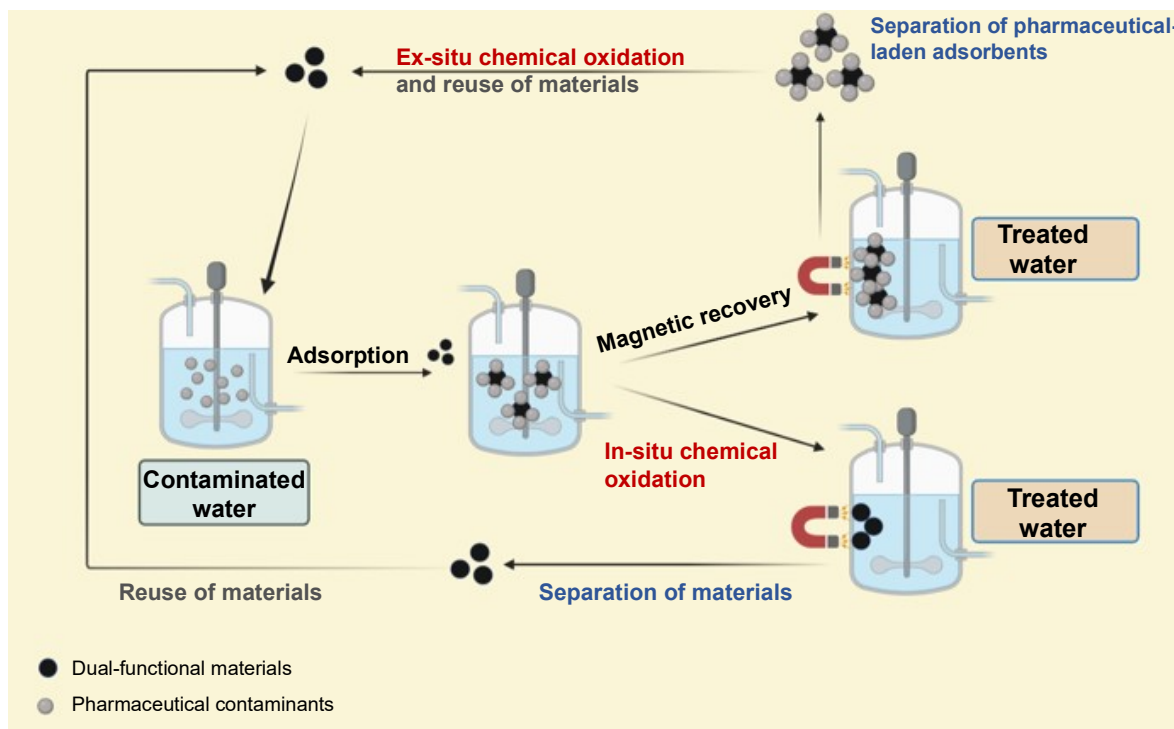
105 further treatment to avoid the risks of secondary contamination. Unlike adsorption, advanced  
106 oxidation processes (AOPs) offer compelling advantage of degrading the organic pollutants.  
107 This feature is highly attractive for environmental protection and to enable decentralized  
108 treatments wherein the collection and transportation of waste are likely to be troublesome [10].  
109 Among AOPs, Fenton-based oxidation processes have received tremendous attention to  
110 degrade pharmaceuticals and other organic pollutants [11]. Heterogeneous Fenton oxidation  
111 relies on iron oxide catalysts to produce reactive oxygen species (ROS predominantly  
112 hydroxyl radicals (HO<sup>•</sup>)) for pollutant degradation. However, Fenton oxidation when applied  
113 alone can be environmentally harmful and expensive due to substantial chemical input [1]. To  
114 overcome these challenges, dual-functional materials are increasingly studied as  
115 heterogeneous catalysts and adsorbents [8, 9]. These materials have the potential to  
116 simultaneously adsorb pollutants (separation-based removal) and catalyze Fenton oxidation  
117 (degradation-based removal). The dual functionality of these materials enables the coupling  
118 of adsorption and Fenton oxidation for higher treatment efficiency while reducing the  
119 associated costs and limitations of individual techniques (by regeneration of materials and  
120 higher elimination of pollutants). Heterogeneous Fenton processes can be further enhanced  
121 with additional input of light (photo-Fenton) that has also been explored. These integrated  
122 treatments can be used for both ex-situ (after separating the adsorbent) as well as in-situ  
123 applications (without separating the adsorbent) by relying on the same materials (Figure 1).  
124 This can be achieved either by using a single material having both functions or by  
125 compositing/impregnating different materials to develop the dual functionality in a hybrid  
126 material. This dual functionality has been the subject of huge amount of research in the recent  
127 decade (Table 1 and 2).

128 In integrated processes, adsorption usually accounts for the initial treatment stage to bind  
129 pharmaceuticals which are then degraded by the ROS formed during Fenton oxidation.  
130 Pollutant adsorption on the surface of dual-functional materials improves the  
131 pollutant/catalyst/oxidant contact which enhances the treatment efficiency. Moreover, the  
132 degradation of adsorbed pharmaceuticals by subsequent Fenton oxidation allows the

133 regeneration of the spent material for further treatment cycles. This regeneration and reuse of  
134 materials are highly advantageous to reduce the treatment cost and to avoid the generation  
135 and disposal of pollutant-laden spent adsorbent. Dual functionality of these materials improves  
136 the pharmaceutical degradation while reducing the risks of secondary contamination [12]. The  
137 disposal of pollutant-laden spent adsorbent is addressed by subsequent Fenton oxidation  
138 that regenerates the adsorbent by removing the pollution. However, in another procedure,  
139 Fenton oxidation can be applied as the initial treatment which is followed by adsorption. This  
140 procedure allows the elimination of the major organic contaminants by Fenton oxidation and  
141 the further removal of their traces and/or byproducts by subsequent adsorption [13, 14]. Thus,  
142 integrated treatments combine the benefits of both techniques. These treatments have,  
143 therefore, distinct advantages of higher contaminant removal, less oxidant consumption and  
144 prevention of secondary pollution.

145 There exist many reviews that focused on the removal of pharmaceuticals from aqueous  
146 environments. However, main focus of these reviews was either various techniques for  
147 pharmaceutical removal [1, 2], Fenton oxidation [15, 16], adsorption [9], or with a focus on  
148 particular group of adsorbents for example sewage sludge-derived biochar [17], carbon  
149 nanotubes [18]. The integration of both processes using dual-functional materials has,  
150 however, not been reviewed so far which constitutes the main objective of this article. To our  
151 knowledge, this is the first review that focuses on the integration of both treatments by relying  
152 on dual-functional materials to eliminate pharmaceutical contaminants from aqueous systems.  
153 For this, we compiled the research data from numerous publications (retrieved from Scopus  
154 database) evaluating the applications of integrated treatments to eliminate pharmaceuticals in  
155 aqueous systems. Dual functionality of iron minerals and their composites with other materials  
156 allows the coupling of adsorption with heterogeneous Fenton and photo-Fenton oxidation  
157 processes. A brief account of the role of these iron minerals in photo-catalysis is also provided.  
158 A critical evaluation of these techniques and materials is provided to demonstrate the  
159 promising treatments/materials with a concise explanation of associated limitations and their  
160 key solutions. With this review, we intend to offer a useful resource and potential research

161 directions to explore the practical implications of Fenton-based processes and adsorption for  
162 real wastewater treatment plants.



163

164 **Figure 1:** The coupling of adsorption and Fenton oxidation by relying on dual-functional  
165 magnetic metal oxide based materials. Adsorption is followed by chemical oxidation to  
166 degrade organic contaminants either after separating the contaminant-laden adsorbents (to  
167 reduce the contamination volume for ex-situ chemical oxidation) or without separating the  
168 adsorbents (in-situ oxidation). In the later system, chemical oxidant is introduced directly in  
169 the same reaction medium that generates the clean adsorbents for their reuse. This figure is  
170 created using Biorender App.

171

## 172 2. Literature Search Methodology

173 Scopus database was searched (on November 21, 2021, updated on June 5, 2022) by using  
174 these keywords in manuscript titles, abstracts, and keywords TITLE-ABS-KEY: ( "Fenton"  
175 AND ( "adsorption" OR "sorption" ) AND ( "pharmaceutical\*" OR "antibiotic\*" OR "personal  
176 care products" ) ). This search procedure is commonly used in bibliometric studies where the  
177 exact phrases are found by using quotation marks ("" ) which deactivate the synonym feature  
178 of search database [11, 19]. Term "or" allows finding various expressions which were coupled  
179 by using "and" to ensure the appearance of these words in the TITLE-ABS-KEY of each article.  
180 The use of asterisk symbol (\*) serves as a wildcard to find the different variations among the



181 target keywords in the databases. For example, the use of “antibiotic\*” allows to find  
182 “antibiotic”, “antibiotics”, or other variations of this term. This search returned 238 articles  
183 which were read to find if it deals with the use of integrated treatment to remove  
184 pharmaceuticals.

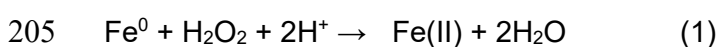
### 185 **3. Coupling of Heterogeneous Fenton oxidation with adsorption**

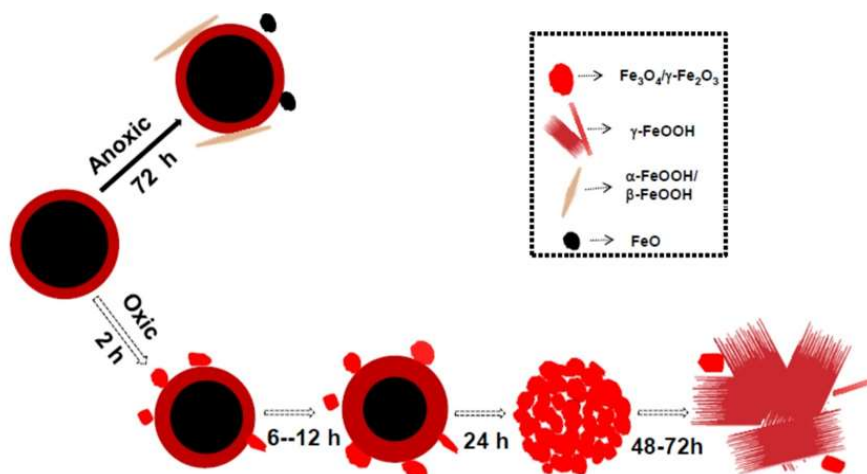
186 Traditional Fenton oxidation counts on dissolved iron species (Fe(II) mainly) to catalyze  
187 hydrogen oxide (H<sub>2</sub>O<sub>2</sub>) for the generation of HO· radicals that degrade organic pollutants.  
188 However, the traditional Fenton process suffers from fundamental drawbacks of maintaining  
189 an acidic pH. The HO· radical production is efficient only at an acidic pH (below 4) which is  
190 costly and impractical in environmental settings [11]. Moreover, this process leads to the  
191 generation of iron sludge after the treatment. To address these drawbacks, heterogeneous  
192 Fenton oxidation has been developed that relies on iron-bearing minerals or solids instead of  
193 dissolved Fe(II). These iron-bearing minerals and solids can catalyze Fenton oxidation at wide  
194 range of pH values [20]. In addition to their catalytic ability, hydrophilic iron oxides also benefit  
195 from their capacity to adsorb polar and negatively charged compounds highlighting their dual  
196 role in the remediation of pharmaceuticals [8, 9]. A brief description of adsorption coupled with  
197 heterogeneous Fenton oxidation using various materials for the removal of pharmaceuticals  
198 is provided below (Table 1).

199

#### 200 **3.1. Pristine nano zero-valent iron (nZVI) and its composites with other materials**

201 Nano zero-valent Fe (nZVI) represents an important material that has been widely used to  
202 promote the integrated remediation processes. Here, the removal mechanism involved the  
203 adsorption of pharmaceuticals on nZVI surface followed by the production of HO· radicals by  
204 its reaction with H<sub>2</sub>O<sub>2</sub> (Eqs. 1 and 2) for pollutant oxidation [21, 22].



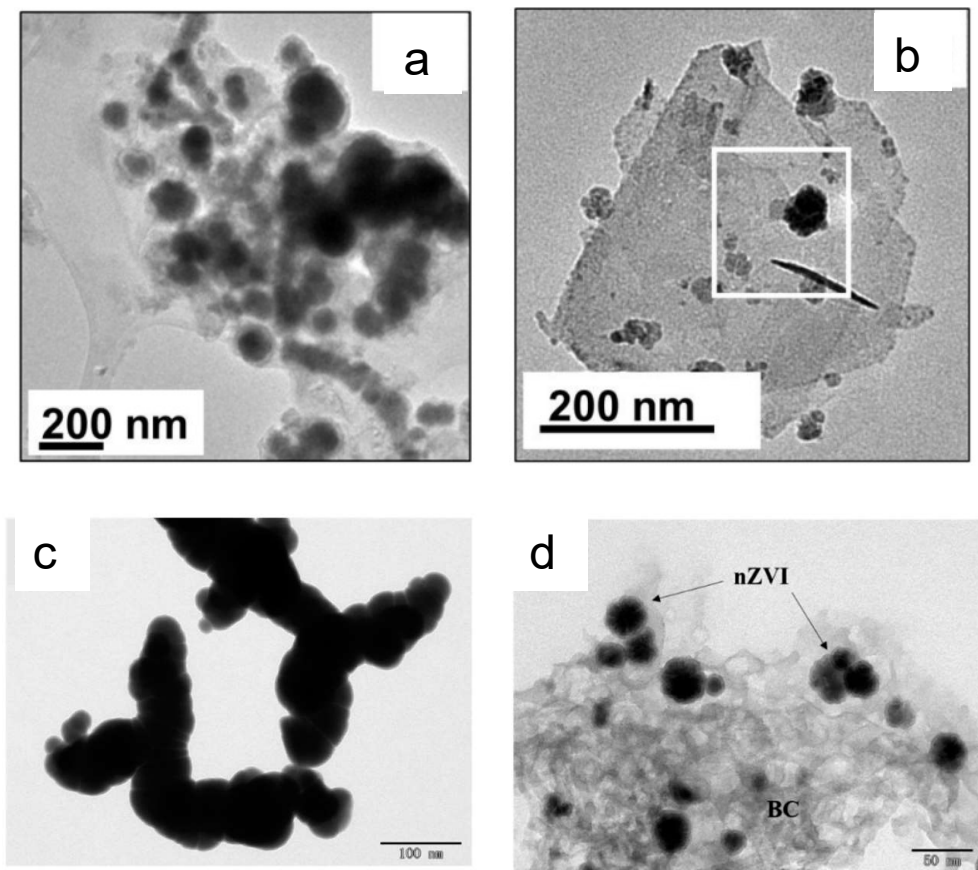


207  
208  
209

210 **Figure 2:** Conceptual model on the passivation evolution of nZVI in water showing the main  
211 passivation byproducts. Reproduced with permission from Ref. [23].  
212

213 Though nZVI particles are highly efficient, they, being highly reactive, are easily oxidized to  
214 form oxide layers on its surface which decreases their catalytic ability (Figure 2) [24]. Indeed,  
215 the surface passivation of NZVI has been recognized among the major challenges in its  
216 successful application to remove pollutants [23, 25]. nZVI corrosion phenomenon is dictated  
217 by various factors including the composition of NZVI itself, oxic/anoxic environments, reaction  
218 time, and the concentration and type of aqueous species [25]. As such, nZVI can be corroded  
219 and transformed into other iron oxides like ferrihydrite, magnetite, etc. which can also  
220 contribute in adsorption and/or Fenton oxidation (Figure 2) [26]. Another issue is the magnetic  
221 nature of nZVI particles that can cause them to spontaneously agglomerate decreasing their  
222 total surface area and efficiency. To address these drawbacks associated with nZVI as dual  
223 functional materials, the stability and reactivity of nZVI particles can be improved by three main  
224 strategies including (i) the development of bimetallic nanocomposites [24, 27], (ii) by loading  
225 nZVI onto a support [22, 28, 29], or (iii) by encapsulating of nZVI particles, for example in  
226 three-dimensional graphene network [30]. These strategies improve the stability and reactivity  
227 of nZVI while reducing its agglomeration. For example, TEM images of nZVI on various  
228 supports indicate its successful attachment preventing its agglomeration (Figure 3). However,  
229 pristine nZVI without any support (Figure 3) exhibits particle agglomeration and the presence

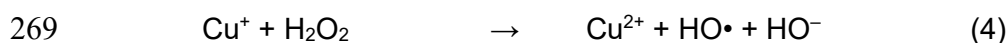
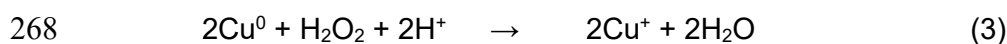
230 of amorphous layers surrounding nZVI particles. These layers have been recognized of iron  
231 oxide layers formed by nZVI oxidation [25, 31]. Thus, without support, Fe particles become  
232 strongly linked to each other under necklet form. This behavior was, however, not observed  
233 in case of bimetallic or composited nZVI (Figure 3 and 4).



234  
235 **Figure 3:** TEM images of pristine nZVI without (a and c) and with its loading onto their  
236 respective supports including reduced graphene oxide (b) and biochar (d). Images a and b  
237 are reproduced with permission from Ref. [28], while images c and d are reproduced with from  
238 Ref. [22], under an open access Creative Commons CC BY 4.0 license.  
239

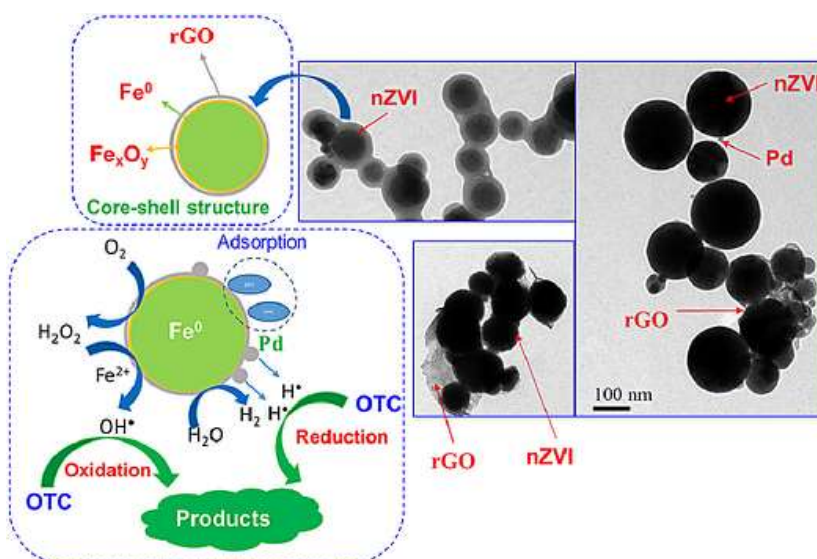
240 Bimetallic nanocomposites can be obtained by adding a second metal to nZVI [24, 27]. For  
241 this, noble metals (e.g. Pt) [24] and other metals (e.g. Cu) [27] were commonly used due to  
242 their significant contribution in enhancing the electron-generation capacity and stability of nZVI  
243 as compared to the pristine nZVI. Moreover, this structural modification largely increased the  
244 surface area from  $25 \text{ m}^2 \text{ g}^{-1}$  (pristine nZVI) to  $300 \text{ m}^2 \text{ g}^{-1}$  (Pt0.5/nZVI). This substantial  
245 increase in the surface area has been marked as the key reason for an improved adsorption  
246 of oxytetracycline by the authors [24]. However, further increase in Pt contents beyond 0.5

247 wt.% turned nZVI particles into flake agglomeration and thus affected the morphology and  
 248 reduced the efficiency of nZVI. Similarly, the use of Cu-based bimetallic nZVI removed 56%  
 249 of ciprofloxacin as compared to pristine nZVI (30% pollutant removal) [27]. In the same study  
 250 [27], an interesting comparison has been made between the efficiency of Cu/nZVI synthesized  
 251 by using green tea extract as the reductant (termed as green method) and the one synthesized  
 252 by traditional chemical method (based on sodium borohydride). Green synthesized Cu/nZVI  
 253 was found more stable, oxidation resistant and efficient than chemically-synthesized Cu/nZVI  
 254 as the former removed 81% of ciprofloxacin compared to the 56% removal by the later. This  
 255 has been linked to the higher dispersion of Cu/nZVI synthesized by green method. Adsorption  
 256 or Fenton-like oxidation alone were able to remove about 30 and 50%, respectively. However,  
 257 the integration of both processes removed up to 90% of ciprofloxacin. Authors further reported  
 258 that adsorption played a major role in pollutant removal in the start of the reaction, but after 5  
 259 minutes, desorption started happening with the passage of time due to surface oxidation of  
 260 nZVI. However, after 20 minutes of reaction, Fenton oxidation began to take over adsorption  
 261 [27]. The stabilization and efficiency of nZVI/Cu bimetallic particles can be further improved  
 262 by polyvinylpyrrolidone [32]. Owing to their catalytic potential of Cu species in promoting  
 263 Fenton oxidation, nano-zerovalent copper ( $\text{Cu}^0$ ) has also been developed as an alternative of  
 264 nZVI to catalyze iron-free Fenton-like oxidation of ciprofloxacin (Equation 3 and 4) [33]. Also,  
 265 the substitution of Cu in  $\text{Fe}_3\text{O}_4$  ( $\text{Fe}_{3-x}\text{Cu}_x\text{O}_4$  as the final product) has been found to increase  
 266 adsorption capacity and  $\text{HO}\cdot$  radical production during photo-Fenton oxidation of anticancer  
 267 drugs including 5-fluorouracil and cyclophosphamide [34].



270 Another strategy to improve the stability of nZVI involves the deposition of nZVI particles on a  
 271 support like biochar [22], reduced graphene oxide [28, 29, 31], cerium oxide [35] etc. which  
 272 can improve its stability and efficiency (Figure 3). For example, the composites of rGO with  
 273 bimetallic Pd/nZVI nanoparticles or nZVI particles provided a good solution to address the  
 274 drawbacks of nZVI based-materials and improved their efficiency [31] (Figure 4). In

275 comparison with 53% removal of oxytetracycline by pristine nZVI, pollutant removal reached  
276 83% with bimetallic Pd/nZVI. Pollutant removal improved to 96% with bimetallic  
277 nanocomposites of Pd/nZVI/rGO5 (rGO 5% w/w). The removal of oxytetracycline by  
278 Pd/nZVI/rGO composite has been linked to adsorption, Fenton-like oxidation, and reduction  
279 reactions as demonstrated in Figure 4. In addition to an improved efficiency, the use of  
280 Pd/nZVI/rGO5 exhibited better pollutant removal in subsequent treatment cycles.  
281 Oxytetracycline removal by pristine nZVI from 53% to 1% in five oxidation cycles whereas the  
282 efficiency of Pd/nZVI/rGO5 composite retained 18% of removal efficiency [31]. Compositing  
283 nZVI with CeO<sub>2</sub> was also found to improve the efficiency and stability of nZVI [35]. A radical  
284 identification experiment linked it to the remarkable production of HO• radical by  
285 nZVI/CeO<sub>2</sub> composite as the bare nZVI. The CeO<sub>2</sub> improved the catalyst's adsorption  
286 characteristics and electron transfer to improve H<sub>2</sub>O<sub>2</sub> decomposition due to the abundance of  
287 surface oxygen vacancies [35].  
288 The encapsulation of nZVI particles in three-dimensional graphene network has also been  
289 proposed as a potential strategy to enhance the stability and efficiency of nZVI [30]. The  
290 encapsulation of iron-copper bimetallic NPs within the mesoporous carbon shell (FeCu@C)  
291 promoted the catalytic degradation of sulfamethazine [36]. Synergistic catalytic role of Fe and  
292 Cu species improved the formation of HO• radicals by promoting  $\equiv\text{Fe(II)}/\equiv\text{Fe(III)}$  redox cycle  
293 while the presence of carbon increased the adsorption capacity (63% pollutant removal).  
294 Sulfamethazine was completely removed in the integrated process.



295  
296

297 **Figure 4:** TEM images of nZVI, nZVI/rGO composite, and bimetallic Pd/nZVI/rGO5  
298 nanocomposite. This image is reproduced with permission from Ref. [31]. This image clearly  
299 depicts that reduced graphene oxide-supported bimetallic palladium-zero-valent-iron  
300 nanocomposites (Pd/nZVI/rGO) prevented the agglomeration nZVI particles and the existence  
301 of iron oxide-associated amorphous layers surrounding them.

302  
303

### 3.2. Pristine iron minerals having dual functions (adsorption and Fenton catalyst)

304 Iron minerals have received substantial attention for their demonstrated efficiency in promoting  
305 both adsorption and Fenton-based oxidation processes. Owing to the high surface area, iron  
306 minerals have been widely used to adsorb variety of pollutants from contaminated  
307 water/wastewater. Structural Fe contents of these minerals enable them to catalyze Fenton  
308 oxidation at circumneutral pH which is highly advantageous for real scale applications. It  
309 should be noted that classical Fenton oxidation ( $H_2O_2 + \text{soluble Fe(II)}$ ) is often limited by the  
310 acidic pH range required to avoid the precipitation of soluble Fe(II). However, in case of iron  
311 minerals, the entrapment of Fe species within the structure of iron minerals prevents their  
312 precipitation leading to an improved catalytic ability over a wide pH range. This quality of iron  
313 minerals makes them ideal catalysts for heterogeneous Fenton oxidation. Iron minerals exist  
314 in nature as ferric (Fe(III) bearing) or mixed-valent iron minerals (bearing Fe(II) both Fe(III))  
315 [37]. For example, FeOOH-based Fenton-like system showed good capacity (80%) to remove  
316 Roxarsone antibiotic and to adsorb arsenic which has been formed as the by-product of  
317 Roxarone oxidation. Thus, the dual-functionality of FeOOH allowed the degradation of the

318 target pharmaceutical while eliminating the risk of secondary contamination [12]. Similarly,  
319 Weng et al. [26] found that the use of green synthesized Fe NPs for synergetic adsorption and  
320 Fenton-like oxidation removed >90% of ofloxacin and enrofloxacin in a mixed contamination  
321 system. After an initial pre-adsorption, these pharmaceuticals were removed by an oxidative  
322 degradation in the presence of H<sub>2</sub>O<sub>2</sub>. These materials also showed good treatment efficiency  
323 either if they were reused (>60%) or were applied to remove target pharmaceuticals in the real  
324 wastewater (>60%) [26].

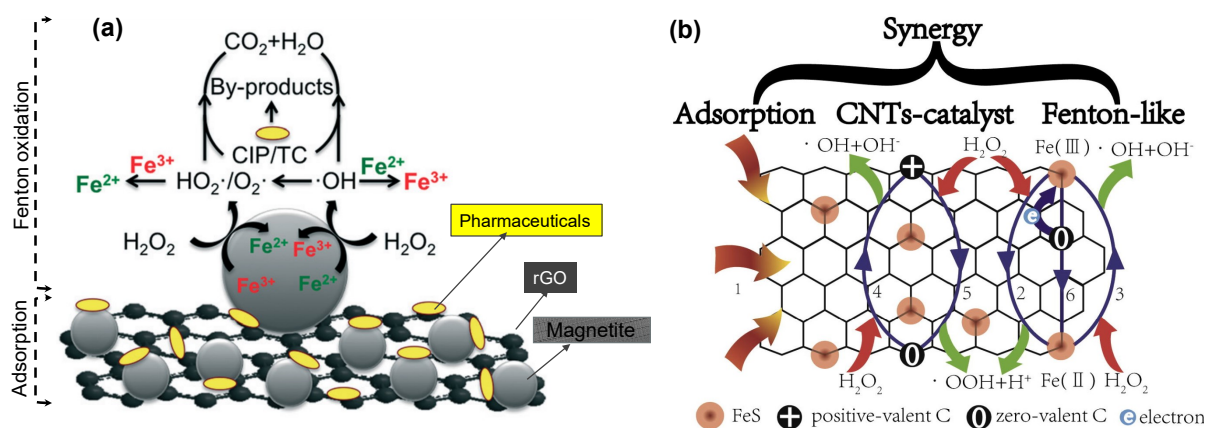
325 Owing to the existence of structural Fe(II), mixed-valent Fe minerals are considered more  
326 reactive to catalyze heterogeneous Fenton oxidation [20]. For example, impregnating  
327 ferrihydrite on powdered activated carbon demonstrated an excellent adsorption capacity (203  
328 mg g<sup>-1</sup>) for diclofenac removal. However, subjecting this material to subsequent Fenton  
329 oxidation partially removed the adsorbed pollutant along with a decrease in its regeneration  
330 ability by 25%. On the other hand, ball-milled magnetite nanoparticles exhibited efficient  
331 removal of ciprofloxacin by heterogeneous Fenton oxidation [38]. Indeed, magnetite alone  
332 removed up to 43% of ciprofloxacin due to adsorption but ciprofloxacin removal was increased  
333 to 89% by subsequent chemical oxidation (H<sub>2</sub>O<sub>2</sub> 12 mM, Fe<sub>3</sub>O<sub>4</sub> 1.75 g L<sup>-1</sup>). It should be noted  
334 that magnetite (Fe(II) Fe(III)<sub>2</sub> O<sub>4</sub>), owing to the presence of structural Fe(II), has emerged as  
335 a viable dual-purpose material that has shown higher catalytic ability as compared to the ferric  
336 minerals [20]. Moreover, its magnetic nature also facilitates the quick recovery of the spent  
337 materials, using an external magnet, from the reaction medium for their reusability or disposal  
338 [39]. The reuse of magnetite in four consecutive treatments by Hassani, et al. [38] revealed  
339 that the efficiency of magnetite decreased from 89% to 65% in four oxidation cycles. The  
340 oxidation efficiency of iron minerals can get decreased by surface oxidation/passivation and  
341 Fe leaching and which, if addressed, can recover the treatment efficiency [19]. The efficiency  
342 and stability of magnetite can be enhanced by preparing its composites with other reactive  
343 materials discussed in following sections.

344

### 345 **3.3. Composites of iron minerals and other materials**

346 The development of efficient composites, particularly based on magnetic materials, has  
347 received tremendous attention in the recent decade. Compositing magnetic iron minerals with  
348 suitable supports can improve the stability and catalytic ability of these iron minerals.  
349 Moreover, composites of magnetic iron minerals with other materials are also prepared to  
350 introduce the magnetic feature in materials which are otherwise deprived of these  
351 characteristics [40-45]. For example, embedding  $\text{Fe}_3\text{O}_4$  nanoparticles on 3D reduced  
352 graphene oxide (rGO) was advantageous to introduce the magnetic feature in the composite  
353 adsorbent and improve the catalytic activity of magnetite [40]. This material ( $\text{Fe}_3\text{O}_4@\text{rGO}$ )  
354 exhibited adsorption capacity ( $2.78 \text{ mmol g}^{-1}$  for ciprofloxacin and  $4.76 \text{ mmol g}^{-1}$  for  
355 tetracycline) much higher than the rGO alone ( $<1 \text{ mmol g}^{-1}$  for both pollutants) and commercial  
356 granular activated carbon ( $<1 \text{ mmol g}^{-1}$ ).  $\text{Fe}_3\text{O}_4$  nanoparticles were deposited between the  
357 graphene sheets and served as spacers preventing the aggregation of graphene sheets. All  
358 the adsorbed amount was completely removed by subsequent Fenton-like oxidation (by  
359 introducing  $\text{H}_2\text{O}_2$ ) and this material maintained its efficiency for 10 adsorption-oxidation cycles  
360 [40]. Total iron loss was only 1% after adsorption-oxidation cycles underscoring the strong  
361 stability and high catalytic efficiency of magnetite nanoparticles on rGO. The existence of both  
362 Fe(II) and Fe(III) in octahedral layer of magnetite on rGO allowed Fe species to be reversibly  
363 oxidized and reduced while retaining the structure [40]. The schematic diagram of this catalytic  
364 oxidation along with iron regeneration is presented in Figure 5a. Similarly, using magnetite  
365 embedded onto chitosan carbon microbeads adsorbed significant amount ( $4.18 \text{ mg g}^{-1}$ ) of  
366 doxycycline under flow through conditions at a flow rate of  $1.1 \text{ mL min}^{-1}$  [46]. Sequential  
367 addition of  $\text{H}_2\text{O}_2$  (5%) to trigger the Fenton oxidation removed up to 95% of the adsorbed  
368 pollutant regenerating the magnetite@chitosan carbon microbeads for repeated applications.  
369 The regeneration efficiency of this magnetic material increased from 78% to 93% of pollutant  
370 removal with an increase in the oxidant dose from 2% to 5% and then decreased to 72% and  
371 55% with further increase in oxidant dose to 8% and 11%. It has been attributed to the  
372 scavenging of  $\text{HO}^\cdot$  radicals at higher oxidant doses [47].





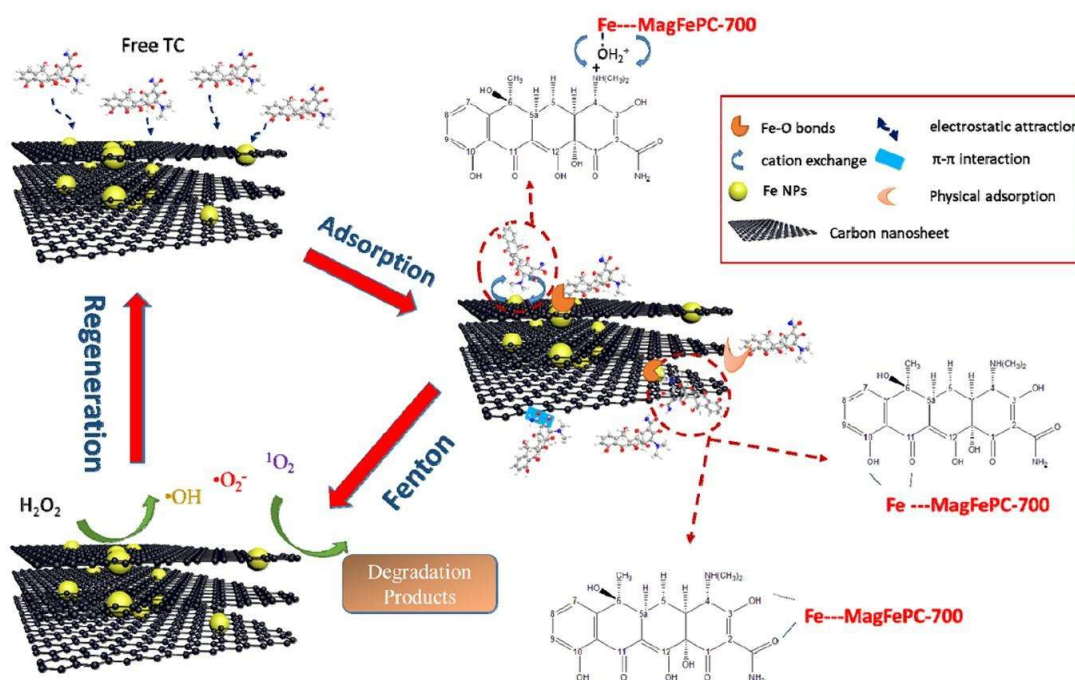
373

374 **Figure 5:** Schematic diagram depicting (a) the removal mechanism of two pharmaceuticals  
 375 (CIP and TC) on the surface of magnetite decorated on 3D reduced graphene oxide (rGO)  
 376 (adapted with permission from Ref. [40]) and (b) removal mechanism of ciprofloxacin by  
 377 Carbon-nanotubes/pyrrhotite catalyst (CNTs/FeS) (reproduced with permission from Ref. [48])  
 378

379 A composite of magnetite with carbon nanotubes (CNTs), synthesized by ball-milling, was  
 380 used to remove six sulfonamides including sulfanilamide, sulfamerazine, sulfadimethoxine,  
 381 sulfadiazine, sulfamethazine, and sulfametoxydiazine [49]. The adsorption efficiency of  
 382 sulfamerazine reached 59%, 70%, and 6% in the presence of magnetite-CNT composite, CNT  
 383 and Fe<sub>3</sub>O<sub>4</sub>, respectively. Though, the adsorption capacity of the composite material was lower  
 384 than CNT, it caused higher pollutant removal by subsequent Fenton oxidation (100%, 71%,  
 385 and 37%, in the presence of magnetite-CNT composite, CNT and Fe<sub>3</sub>O<sub>4</sub>, respectively with  
 386 H<sub>2</sub>O<sub>2</sub>). Moreover, the presence of magnetite introduces the magnetic character in composite  
 387 material that facilitated its separation for regeneration. Carbon-nanotubes (CNTs)/pyrrhotite  
 388 (FeS) also exhibited substantial removal (90%) of ciprofloxacin that has been linked to the  
 389 synergistic adsorption, Fenton-like oxidation and catalytic degradation by CNTs catalyst [48]  
 390 (Figure 5b). CNTs possess excellent adsorption capacity owing to its large surface area and  
 391 porous structure. On the other hand, FeS can produce Fe(II) in solution that would catalyze  
 392 H<sub>2</sub>O<sub>2</sub> to produce HO· radicals for the degradation of ciprofloxacin. Additional trials performed  
 393 using HO· radical scavengers including potassium iodide (surface-bound radical scavenger)  
 394 and methanol (scavenger for all the unbounded HO· radicals) revealed that the removal of  
 395 ciprofloxacin was mainly dependent on unbounded HO· radicals while the contribution of

396 bounded HO<sup>•</sup> radicals remains insignificant. Adsorption process alone was able to remove  
397 25% of ciprofloxacin while the removal efficiency reached 90% in integrated process due to  
398 the synergistic effect of adsorption and oxidation by free and bounded HO<sup>•</sup> radicals.

399 Biochar has also emerged as an important material in the recent decade with many  
400 environmental applications. It can be developed from various biomasses. For example,  
401 biochar [50] or carbon [51], derived from sewage sludge with sufficient amounts of native Fe,  
402 removed pharmaceuticals (90-91%) through synergetic effect of adsorption and Fenton  
403 oxidation. Relying on sewage sludge or agricultural wastes to synthesize biochar could reduce  
404 the treatment cost while offering an innovative solution for solid waste management [52, 53].  
405 However, depending upon the contents and form of iron in biomass, Fe loading on biochar  
406 can be required to improve its catalytic ability. For example, Xie et al. [54] developed  
407 composites of Fe<sub>x</sub>P/biochar by pyrolysis of phosphorus-containing biomass (yeast) preloaded  
408 with FeOOH on its surface. Synergistic adsorption and Fenton-like oxidation removed 99% of  
409 sulfamethoxazole. However, the development of composite materials usually involves  
410 impregnation method where iron precursor-loaded carbon materials are pyrolyzed or iron  
411 oxides are immobilized onto carbon materials. These approaches can be limited by uneven  
412 distribution of iron or its oxides on the surface of composite materials. In this regard, direct  
413 carbonization of metal organic frameworks (MOFs) to synthesize carbon-based porous  
414 materials has been suggested by Gu et al. [55]. They developed a magnetic Fe/porous carbon  
415 material via one-step pyrolysis method and found it highly suitable to remove tetracycline.  
416 Highest adsorption of 1301 mg g<sup>-1</sup> onto this material was recorded which was about 6 times  
417 higher than activated carbon. The mechanism of adsorption mainly included surface  
418 complexation, hydrogen bonding and π–π interactions (Figure 6). Fenton oxidation allowed  
419 the regeneration of this material for further treatment cycles where it retained its efficiency (70-  
420 79%) [55].



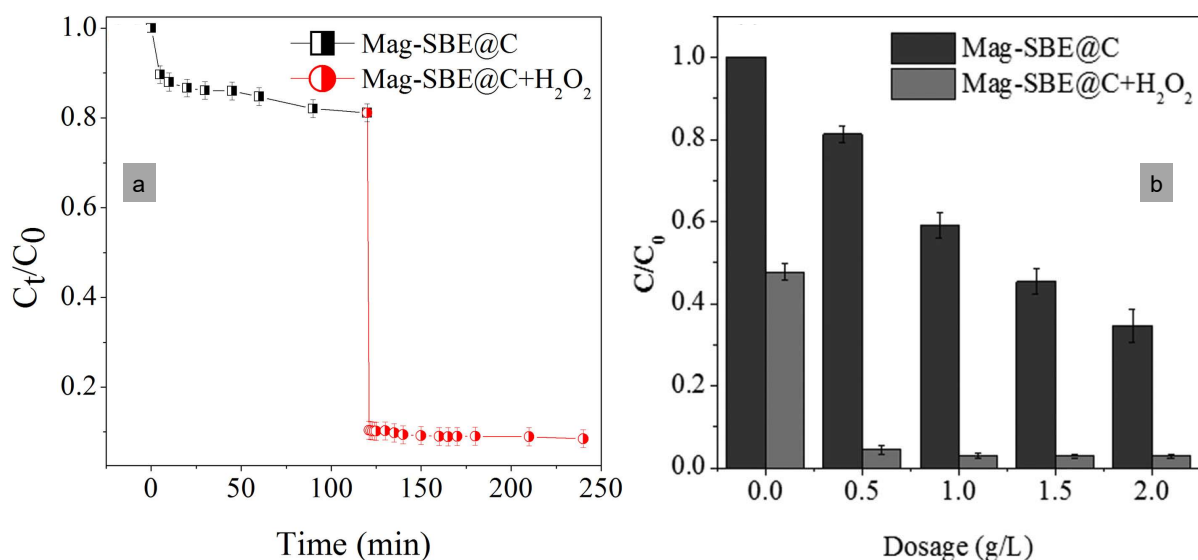
421 **Figure 6:** Mechanisms involving the role of magnetic Fe/porous carbon hybrid for the  
 422 adsorption of tetracycline (TC) followed by Fenton oxidation to regenerate this material. This  
 423 figure is reproduced with permission from Ref. [55].  
 424  
 425

426 Magnetic iron-based carbon materials are also gaining particular interest because of the  
 427 remarkable adsorption from the mutual role of carbon (C) and Fe, higher catalytic ability  
 428 associated mainly with Fe species, and easy recovery from aqueous matrix due to their  
 429 magnetic nature for repeated applications [55-57]. Iron-based MOFs (NH<sub>2</sub>-MIL-88B) were  
 430 found to completely remove pefloxacin from contaminated solution by adsorption followed by  
 431 Fenton-like oxidation [58]. Adsorption capacity reached 41.4 mg·g<sup>-1</sup> in 120 min whereas  
 432 pefloxacin was completely removed by subsequent Fenton-like oxidation. Similarly,  
 433 Fe<sub>2</sub>O<sub>3</sub>@covalent organic frameworks (Fe<sub>2</sub>O<sub>3</sub>@COFs) was synthesized by restricting the  
 434 growth of Fe<sub>2</sub>O<sub>3</sub> in the nanoscale channel of COFs [56]. The use of this material resulted in  
 435 45% removal of sulfamethazine (by adsorption) while integration with H<sub>2</sub>O<sub>2</sub> completely  
 436 removed this pollutant.

437 Recently, magnetic spent bleaching earth carbon was synthesized by the anoxic pyrolysis of  
 438 spent bleaching earth, a waste product of vegetable oil industry, followed by the in-situ  
 439 synthesis of magnetite via coprecipitation [59]. The adsorption of tetracycline hydrochloride  
 440 reached 16% with equilibrium attained in in 60 minutes. Pollutant removal efficiency reached

441 89% after one minute of oxidant addition in the reaction medium (Figure 7a). An increase in  
 442 the quantity of this material from 0.5 to 2 g L<sup>-1</sup> increased the adsorption of tetracycline  
 443 hydrochloride from 18 to 65% and oxidation 52 to 97% (Figure 7). The development of efficient  
 444 environmental materials from solid industrial wastes (like that of spent bleaching earth) could  
 445 be a sustainable solution for resource recovery and solid waste management. However, for  
 446 all the composite materials, maintaining an optimum level of iron loading is crucial to attain the  
 447 maximum degradation of pollutants. Increasing iron loading beyond an optimum point makes  
 448 iron dispersion less homogeneous which reduces the oxidation efficiency [60]. In another  
 449 study, the loading of Fe<sub>3</sub>O<sub>4</sub> on cellulose nanocomposites reduced the iron loss from 19% (from  
 450 Fe<sub>3</sub>O<sub>4</sub>) to <1% (in composite sample) while removing about 90% of tetracycline due to the  
 451 supportive role of adsorption and Fenton-like degradation [61]. It is worth mentioning that  
 452 adsorption alone was able to remove only 33% of tetracycline. Moreover, the development of  
 453 bioinspired magnetic cellulose nanocomposites has been suggested as a suitable alternative  
 454 to the chemically-synthesized supports which are non-degradable, environmentally  
 455 unsustainable or their synthesis relies on hazardous chemicals [61].

456



457

458 **Figure 7:** Removal of tetracycline hydrochloride (a) by adsorption on magnetic spent  
 459 bleaching earth carbon (Mag-SBE@C alone) or in combination with Fenton oxidation (Mag-  
 460 SBE@C + H<sub>2</sub>O<sub>2</sub>), (b) with various dosages of Mag-SBE@C. These images are reproduced  
 461 with the permission from Ref. [59].

462  
463

**Table 1:** Summaries of the studies reporting the integration of adsorption and heterogeneous Fenton oxidation to remove pharmaceuticals in aqueous solutions. Studies are arranged chronologically.

Tested material	Pollutant	Experimental conditions	Removal efficiency	Ref.
CNTs/FeS	Ciprofloxacin (120 mg L <sup>-1</sup> )	Material = 25.5 mg, H <sub>2</sub> O <sub>2</sub> = 10.3 mmol L <sup>-1</sup>	25% removal by adsorption alone while 90% removal with synergistic oxidation	[48]
Ce <sup>0</sup> -Fe <sup>0</sup> -reduced graphene oxide	Sulfamethazine (20 mg L <sup>-1</sup> )	Material = 0.5 g L <sup>-1</sup> , H <sub>2</sub> O <sub>2</sub> = 10 μL, pH = 7, T = 25 °C	100%	[29]
Fe <sub>3</sub> O <sub>4</sub>	Ciprofloxacin (10 mg g L <sup>-1</sup> )	Material = 1.75 g L <sup>-1</sup> , H <sub>2</sub> O <sub>2</sub> = 12 mM, pH = 3	43% removal by adsorption and 88.92% in the presence of oxidant	[38]
FeOOH	Roxarsone (10 mg L <sup>-1</sup> )	Material = 0.1 g L <sup>-1</sup> , pH = 5, T = 20 ± 2 °C, time = 3 h	80% of roxarsone by Fenton oxidation with simultaneous removal of arsenic, byproduct of oxidation, by adsorption in the same setup	[12]
3D-rGO/Fe <sub>3</sub> O <sub>4</sub>	Ciprofloxacin (CIP) and tetracycline (TC) (200 μmol L <sup>-1</sup> each)	Solid = 0.33 g L <sup>-1</sup> pH 6, time = 72 h, Fe <sub>3</sub> O <sub>4</sub> : H <sub>2</sub> O <sub>2</sub> = 1:2 molar ratio	Maximum adsorption of 2.78 mmol g <sup>-1</sup> for CIP and 4.76 mmol g <sup>-1</sup> for TC followed by the complete oxidation of adsorbed pollutant	[40]
Fe <sub>3</sub> O <sub>4</sub> @Chitosan carbon microbeads	Doxycycline (25 mg L <sup>-1</sup> )	pH 7, flow rate: 1.1 mL/min, H <sub>2</sub> O <sub>2</sub> = 5% wt, Flow-through system	Highest adsorption: 4.18 mg g <sup>-1</sup> followed by 93% removal by oxidation	[46]
Sewage sludge biochar	Ciprofloxacin (10 mg L <sup>-1</sup> )	Material = 0.2 g L <sup>-1</sup> , pH 4, H <sub>2</sub> O <sub>2</sub> = 10 mM, time = 4 h	About 30% by adsorption but 90% by integrated system	[50]
FeCu@C composite	Sulfamethazine (20 mg L <sup>-1</sup> )	pH = 3.0, material = 0.25 g L <sup>-1</sup> , [H <sub>2</sub> O <sub>2</sub> ] = 1.5 mM, T = 25 °C.	62% by adsorption alone while 100% removal in integrated process	[36]
Sludge derived carbon	Ofloxacin (30 mg L <sup>-1</sup> )	Material = 1 g L <sup>-1</sup> , H <sub>2</sub> O <sub>2</sub> = 138 mg L <sup>-1</sup> , time = 540 min	91%	[51]
nZVI/CeO <sub>2</sub>	Tetracycline (100 mg L <sup>-1</sup> )	Material = 0.1 g L <sup>-1</sup> , H <sub>2</sub> O <sub>2</sub> = 100 mmol L <sup>-1</sup> , pH = 3, T = 26 °C	93%	[35]
nZVI encapsulated in 3-D graphene network	Sulfadiazine (10 mg L <sup>-1</sup> )	pH 3-4, [H <sub>2</sub> O <sub>2</sub> ] = 3 mM, material = 0.5 g L <sup>-1</sup> , T = 298 K	81% by adsorption alone and 98% in integrated process	[30]
nZVI/Cu composites	Ciprofloxacin (50 mg L <sup>-1</sup> )	GT-nZVI/Cu (1/0.08) = 0.5 g L <sup>-1</sup> , pH = 5, T = 293 K H <sub>2</sub> O <sub>2</sub> generated in-situ	30 and 50% removal by adsorption or Fenton-like oxidation, respectively. 90% removal by integrated process	[27]
Pt/nZVI nanocomposites	Oxytetracycline (100 mg L <sup>-1</sup> )	Pt0.5/nZVI = 0.3 g L <sup>-1</sup> , pH = 5, H <sub>2</sub> O <sub>2</sub> generated in-situ	99%	[24]
rGO-nZVI nanohybrids	12 pharmaceuticals including antibiotic, anti-inflammatory, anti-seizure, and	t = 10 min, H <sub>2</sub> O <sub>2</sub> (15.6 μL, 28-30%), solution vol = 15 mL, Material = 530 mg L <sup>-1</sup>	95-99%	[28]

	antidepressants (200 $\mu\text{g L}^{-1}$ each)			
nZVI-biochar composites	Ornidazole (100 $\text{mg L}^{-1}$ )	pH = 3, T = 25 °C, $[\text{H}_2\text{O}_2] = 12 \text{ mM}$ , nZVI-Biochar = 0.3 $\text{g L}^{-1}$ (mass ratio of 1:2)	80%	[22]
Mussel-inspired magnetic cellulose nanocomposite	Tetracycline (20 $\text{mg L}^{-1}$ )	Material = 100 $\text{mg L}^{-1}$ $\text{H}_2\text{O}_2 = 0.10 \text{ M}$ , T = 308.15 K	33% by adsorption and 90% by the integrated system	[61]
nZVI loaded MOF MIL-101(Cr)	Tetracycline	Material = 0.25 $\text{g L}^{-1}$ , $\text{H}_2\text{O}_2 = 0.10 \text{ M}$ pH = 3 – 7, $\text{H}_2\text{O}_2 = 50 \text{ mM}$ , time = 60 min	Adsorption capacity was 625 $\text{mg g}^{-1}$ , 93% removal by Fenton oxidation	[62]
$\text{Fe}_x\text{P}$ /biochar	Sulfamethoxazole (20 $\text{mg L}^{-1}$ )	Material = 0.4 $\text{g L}^{-1}$ , T = 30 °C, $\text{H}_2\text{O}_2$ generated in-situ	99%	[54]
Magnetic Cellulose Nanocomposites	Tetracycline (100 $\text{mg L}^{-1}$ )	Time = 60 min, material = 0.2 $\text{g L}^{-1}$ ,	90% in integrated system while 33% with adsorption alone	[61]
Green synthesized Fe NPs	Ofloxacin & enrofloxacin (50 $\text{mg L}^{-1}$ each)	Material = 0.8 $\text{g L}^{-1}$ ; pH = 7.1; T = 25 °C; $\text{H}_2\text{O}_2 = 40 \text{ mM}$	90-91% for both pollutants	[26]
Fe-modified zeolite	Tartrazine (10 $\text{mg L}^{-1}$ )	Material = 50 $\text{g L}^{-1}$ $[\text{H}_2\text{O}_2] = 2 \text{ mM}$ , pH = 3 and T = 20 °C	85% by adsorption while 95% degradation by subsequent oxidation	[63]
Leather waste derived biochar	Sulfamethoxazole (20 $\text{mg L}^{-1}$ )	Continuous mode, Material = 20 $\text{mg L}^{-1}$ , $\text{H}_2\text{O}_2 = 10 \text{ mM}$ , pH = 3.0, current velocity = 3.5 mL/min	90% by adsorption and subsequent Fenton oxidation completely regenerated the material	[64]
$\text{FeNi}_3$ nanoparticles	Metronidazole (10 $\text{mg L}^{-1}$ )	Time = 180 min, Material = 0.005 $\text{g L}^{-1}$ , and $[\text{H}_2\text{O}_2] = 150 \text{ mg L}^{-1}$	45% by adsorption and 100% by subsequent oxidation	[65]
$\text{Fe}_2\text{O}_3$ @covalent organic frameworks	Sulfamethazine (10 $\text{mg L}^{-1}$ )	Material = 1 $\text{mg L}^{-1}$ , T = 25 °C, pH = 3, $\text{H}_2\text{O}_2 = 2.6 \text{ mM}$	45% by adsorption and 100% by integration with oxidation	[56]
Poly(aspartic acid) $\text{Fe}_2\text{O}_3$ - $\text{MnO}_2$ micromotor	Tetracycline (30 $\text{mg L}^{-1}$ ) with Pb and Cd	Time = 50 mins, $\text{H}_2\text{O}_2 = 3\%$ , material = 80 $\text{mg L}^{-1}$	83% removal of tetracycline and 25% removal of metal mixture by integrated treatment	[66]
Magnetic spent bleaching earth carbon	Tetracycline (0.7 $\text{mmol L}^{-1}$ )	Material = 1.0 $\text{g L}^{-1}$ T = 41 °C, pH = 4.89 and molar ratio of $\text{H}_2\text{O}_2$ to pollutant = 277	19% by adsorption and increased to 91% with oxidation	[59]
rGO- supported bimetallic Pd/nZVI nanocomposites	Oxytetracycline (100 $\text{mg L}^{-1}$ )	Material = 0.1 $\text{g L}^{-1}$ (5% rGO), pH = 5.0 and T = 25 °C	53%, 83% and 96% pollutant removal efficiency by pristine nZVI, bimetallic Pd/nZVI, and bimetallic nanocomposites of Pd/nZVI/rGO5, respectively	[31]

Composite of magnetite with carbon nanotubes	Sulfonamides (40 mg L <sup>-1</sup> )	Material = 1 g L <sup>-1</sup> , H <sub>2</sub> O <sub>2</sub> = 24.5 mM, pH = 3	100% removal in the integrated system while 59% by adsorption alone	[49]
Magnetic Fe/porous carbon hybrid	Tetracycline (80 mg L <sup>-1</sup> )	Material = 0.05 g L <sup>-1</sup> ; equilibrium pH = 6; T = 25 °C	Adsorption capacity of 1301 mg g <sup>-1</sup> , Fenton oxidation regenerated the material while removing the pollution.	[55]
Fe-based MOF, NH <sub>2</sub> -MIL-88B	Pefloxacin (20 mg L <sup>-1</sup> )	pH = 6.0, Material = 0.5 g L <sup>-1</sup> , [H <sub>2</sub> O <sub>2</sub> ] = 8.0 mmol L <sup>-1</sup> , T = 30 °C	Adsorption of 41.37 mg·g <sup>-1</sup> , with >99% removal by Fenton oxidation	[58]
Mn-CuO	Ciprofloxacin (10 mg L <sup>-1</sup> )	H <sub>2</sub> O <sub>2</sub> = 40 mmol L <sup>-1</sup> ; pH = 5.3, material = 1 g L <sup>-1</sup> , time = 90 minutes	<20% pollutant removal by adsorption while integration with oxidation removed about 80%.	[67]
Fe <sub>3</sub> O <sub>4</sub> @ZIF-8@ZIF-67 nanocomposite	Tetracycline (160 mg L <sup>-1</sup> )	material = 0.4 g L <sup>-1</sup> , H <sub>2</sub> O <sub>2</sub> = 30 mM, T = 25 °C	89% by adsorption alone while 96% by integrated process	[68]
Pyrite nanosheets	Ciprofloxacin (20 mg L <sup>-1</sup> )	pH = 4, H <sub>2</sub> O <sub>2</sub> = 2 mmol L <sup>-1</sup> , material = 1 g L <sup>-1</sup> , time = 10 min	20% removal by adsorption and complete removal by subsequent oxidation	[69]

464

#### 465 **4. Coupling of photo-Fenton and photocatalysis with adsorption**

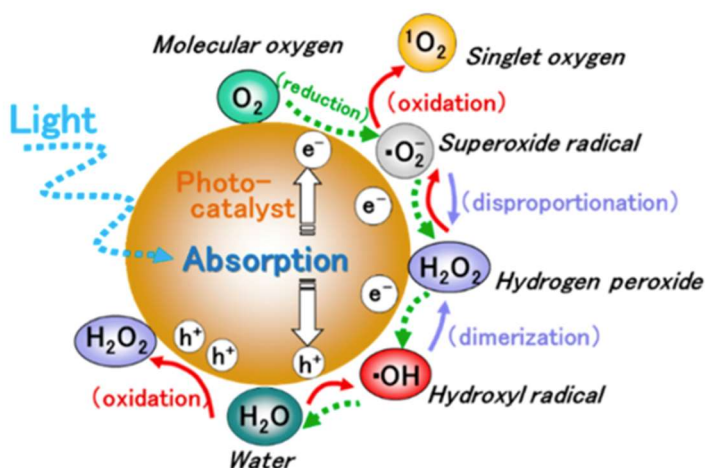
466 Photo-induced processes including photo-Fenton and photocatalysis can be employed in  
467 combination with adsorption to remove pharmaceutical compounds. Compared to the  
468 traditional Fenton and Fenton-like processes, photo-Fenton involves the photo-reduction of  
469 iron(III) to generate ROS under light, especially HO<sup>•</sup> radicals (Equation 5). Photo-Fenton  
470 reaction favors the regeneration of Fe(II) that addresses the rate limiting step of Fenton  
471 oxidation (reduction of iron(III) into iron(II)) [70, 71]. The use of Fe(III) is a considerable  
472 advantage since it is more stable than Fe(II) at circumneutral pH. In addition, H<sub>2</sub>O<sub>2</sub> can be also  
473 added to the photo-Fenton process, so classical Fenton reaction occurs. Therefore, a catalytic  
474 cycle Fe(III) ↔ Fe(II) is set up.



476 Photo-Fenton oxidation and adsorption are usually integrated using composite materials  
477 based on iron oxides composited with different adsorbents (Table 2). Consequently, the  
478 composite materials can also trigger photocatalysis in the case the iron-based material is a  
479 semiconductor [72-74]. Photocatalysis relies on the formation of electron-hole ( $e^-/h^+$ ) pairs  
480 under light which react further to generate primary ROS (Figure 8). It is worth noting that the  
481 isolated use of photo-Fenton/photocatalysis and adsorption processes has been widely  
482 studied. However, their simultaneous application is an emerging field with relatively fewer  
483 studies. This section illustrates the integration of adsorption with photo-Fenton and  
484 photocatalysis for the removal of pharmaceuticals. A brief summary of the salient findings  
485 regarding the efficiency of various materials in integrated processes is provided in Table 2. A  
486 brief description of these studies is provided in the following sections.

487





488

489 **Figure 8:** Photocatalytic generation of primary reactive oxygen species (ROS) *via*  
 490 photocatalytic reduction and oxidation steps of oxygen and water. This figure is reproduced  
 491 with permission from Ref [75].

492

#### 493 **4.1. Iron-based materials combined with zeolites and porous alumina**

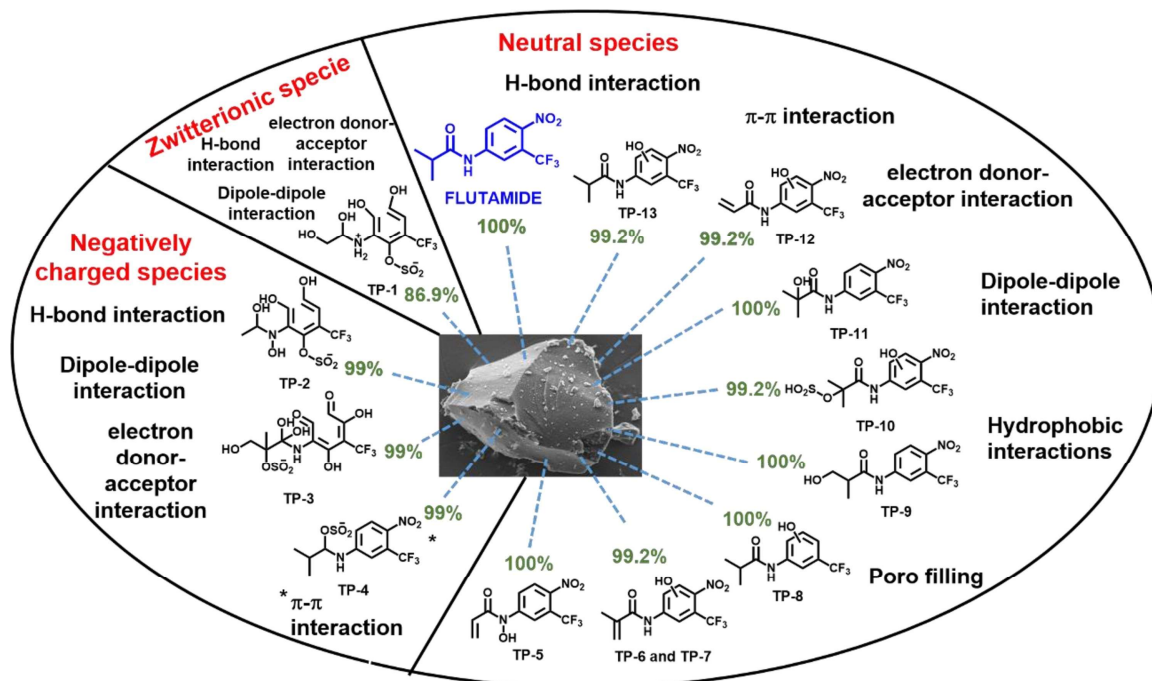
494 Iron-based spinel structure are widely used photoactive materials, especially for  
 495 heterogeneous photo-Fenton process. Their combination with zeolite showed promising  
 496 potential to remove pharmaceutical compounds since zeolites exhibit excellent adsorption  
 497 properties due to high ion exchange properties, hydrophilic affinities and specific surface area  
 498 [76, 77]. Indeed, NaX nanozeolite combined with  $\text{CoFe}_2\text{O}_4$  can completely remove  
 499 paracetamol ( $20 \text{ mg L}^{-1}$ ) after 30 min irradiation under UVA light in the presence of  $\text{H}_2\text{O}_2$ , that  
 500 corresponds to a 50% increase in pollutant removal extent compared to that by adsorption  
 501 alone [77]. Such a high efficiency is due to the synergy of iron-based catalyst and zeolites,  
 502 owing to their excellent adsorption capacity and hydrophilic affinities. Higher adsorption  
 503 improves the contact of paracetamol with the iron-based catalyst enhancing its degradation  
 504 with photo-Fenton process [76, 77]. Similarly, mesoporous alumina is an excellent adsorbent  
 505 for the support of photo-Fenton catalyst. Indeed, the combination of meso- $\text{Al}_2\text{O}_3$  with Fe(II)  
 506 can almost completely remove phenol after 60 min in the presence of  $\text{H}_2\text{O}_2$  under UV light at  
 507 pH = 3 [78]. Adsorption alone can remove 40% of phenol due to the high chemical and thermal  
 508 stability of mesoporous alumina along with its high specific surface area. The integration of

509 adsorption with photo-Fenton process leads to an increase of 60% in degradation extents  
510 owing to the oxidative attack of hydroxyl radicals on phenol.

#### 511 **4.2. Iron-based materials combined with biomass-based adsorbents**

512 Biomass-based materials, particularly activated carbon, are considered highly promising due  
513 to their natural origin and their sustainable production. Recently, Della-Flora et al. designed  
514 an integrated adsorption system with photo-Fenton process to remove a mixture of  
515 pharmaceutical compounds (to simulate hospital wastewater) including chloramphenicol,  
516 fluconazole, flutamide, furosemide, gemfibrozil, ibuprofen, losartan, nimesulide and  
517 paracetamol [13, 79]. The first step involves the photo-Fenton process which is performed for  
518 15 min under simulated solar light at pH = 4 with a single addition of 100 mg L<sup>-1</sup> H<sub>2</sub>O<sub>2</sub> and  
519 multiple additions of Fe(II) (5 mg L<sup>-1</sup> at 0 min, 5 min and 10 min of treatment time).  
520 Subsequently, adsorption process using activated carbon obtained from avocado seeds is  
521 performed as post-treatment for 15 min. Such a combination of processes can remove almost  
522 completely all the pharmaceutical compounds. Indeed, the photo-Fenton process can degrade  
523 from 30% to 80% of the contaminant after 15 min (depending upon pharmaceutical  
524 compound), and the remaining contamination including the toxic transformation products can  
525 be removed by adsorption. There exist multiple adsorption reactions as illustrated in Figure 9  
526 with the example of flutamide in the presence of activated carbon from avocado seeds [69].  
527 However, the involvement of photo-Fenton process requires the acidification of the water  
528 matrix which is not economically viable [70, 71]. In addition, the pH also affects the efficiency  
529 of adsorption process through activated carbon [13]. At acidic pH, the chemical structure of  
530 the adsorbent is composed of aromatic rings, possesses positively charged surface. Thus  
531 most of the target and transformed pharmaceutical compounds, which also contain aromatic  
532 rings and are neutral or negatively charged at acidic pH, are easily adsorbed through  
533 Coulombic and π-π interactions [13]. It is worth noting that the open-ring transformation  
534 products are not efficiently removed by adsorption process due to weak interactions with the  
535 adsorbent and strong solubility in water, respectively, but the photo-Fenton process can

536 efficiently degrade and mineralize this fraction of the contamination [13, 79]. These studies  
 537 highlight the utility of the adsorption as the secondary process in the integrated system.



538  
 539 **Figure 9:** Characterization of activated carbon by scanning electron microscopy and  
 540 description of proposed adsorption mechanisms and interaction of Flutamide  
 541 transformation products after solar photo-Fenton oxidation in hospital wastewater. \*  
 542 represents the percentage of the abundance of each specie at pH 4. This figure is reproduced  
 543 with permission from Ref. [13].  
 544

545 Another integrated system combining adsorption and photo-Fenton processes has been  
 546 discussed by Oladipo et al. where tetracycline and phenol have been removed using Fe<sub>3</sub>O<sub>4</sub>  
 547 nanoparticles covered by waste *Cyprus* coffee residue (Fe<sub>3</sub>O<sub>4</sub>@CC) [72]. Such a composite  
 548 can adsorb tetracycline with an increase of 50% compared to CC alone and degrade and  
 549 mineralize efficiently this pharmaceutical compound along with its aromatic intermediates in  
 550 the presence of H<sub>2</sub>O<sub>2</sub> and solar irradiation [72]. As expected, the excellent adsorption capacity  
 551 of Fe<sub>3</sub>O<sub>4</sub>@CC was found dependent on the solution pH. Tetracycline exists in cationic form at  
 552 pH < 3.3, in anionic form at pH > 7.7, and as zwitterion between pH 3.3 and 7.7. Therefore,  
 553 the optimal adsorption of tetracycline occurred at circumneutral pH and it is due to electrostatic  
 554 interactions and H-bonding between the waste coffee residue and the iron oxide, respectively,  
 555 and the pharmaceutical compound [72]. The photo-Fenton process generated ROS (mainly

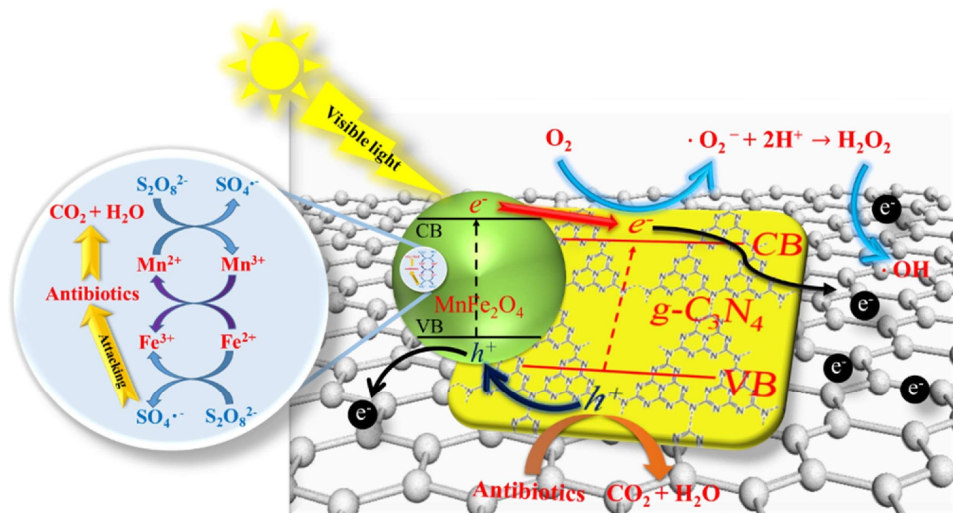
556 HO<sup>•</sup> and O<sub>2</sub><sup>•-</sup>/HO<sub>2</sub><sup>•</sup>), that efficiently degraded tetracycline as well as its degradation byproducts  
557 such as phenol, catechol and hydroquinone [72]. Therefore, the use biomass-based adsorbent  
558 including activated carbon in integrated adsorption with photo-Fenton system is an interesting  
559 strategy for the efficient removal of pharmaceutical compounds. Such adsorbents interact with  
560 aromatic contaminants by π-π- and H-bonding, while photo-Fenton process efficiently oxidize  
561 the remaining pollution in the solution.

562

### 563 **4.3. Iron-based materials combined with g-C<sub>3</sub>N<sub>4</sub>**

564 The integration of adsorption with both photo-Fenton and/or photocatalysis has also been  
565 proposed as an innovative system [80, 81]. Indeed, iron-based oxides can also play the role  
566 of photocatalyst and adsorbent for the removal of pharmaceuticals. For instance, the  
567 composites based on graphitic carbon nitride (g-C<sub>3</sub>N<sub>4</sub>) and, iron-based oxide (like Fe<sub>2</sub>O<sub>3</sub> and  
568 MnFe<sub>2</sub>O<sub>4</sub>) belong to such an integrated system [80, 81]. Eventually, an adsorbent can also be  
569 included in the composite like graphene [80]. For example, *Zhao et al.* investigated a  
570 composite material made of g-C<sub>3</sub>N<sub>4</sub> with Fe<sub>2</sub>O<sub>3</sub> nanodots [81]. Such a composite can degrade  
571 90% of tetracycline in the presence of H<sub>2</sub>O<sub>2</sub> after 1 h under visible light. For comparison, the  
572 integrated adsorption with photocatalysis (without H<sub>2</sub>O<sub>2</sub>) and Fenton process (in the dark) can  
573 only degrade about 20% and 45% of the target pharmaceutical, respectively [81]. However,  
574 the photo-Fenton is not discussed in detail by *Zhao et al.*, although it has probably a significant  
575 contribution to the excellent efficiency of the g-C<sub>3</sub>N<sub>4</sub>/Fe<sub>2</sub>O<sub>3</sub> composite. It is also worth noting  
576 the g-C<sub>3</sub>N<sub>4</sub>/Fe<sub>2</sub>O<sub>3</sub> composite is highly stable since the efficiency of tetracycline degradation by  
577 integrated adsorption with simultaneous photocatalysis and photo-Fenton decreased by about  
578 4% after 4 repeated runs. On the other hand, *Wang et al.* [80] prepared g-  
579 C<sub>3</sub>N<sub>4</sub>@MnFe<sub>2</sub>O<sub>4</sub>@graphene composites for the degradation of a wide range of antibiotic  
580 compounds including tetracycline, ciprofloxacin, metronidazole and amoxicillin. Such  
581 composites integrate a non-photoactive adsorbent, thus combining photocatalysis, photo-  
582 Fenton and adsorption (Fig. 10). The photochemical systems also included the use of

583 persulfate ( $S_2O_8^{2-}$ ) as radical precursor. The pollutant degradation efficiency ranged from 50%  
 584 to 90% in 10 mM pharmaceutical solutions after 90 min visible light irradiation (depending  
 585 upon the compound) [80]. In addition, the reusability of such composites is excellent as no  
 586 significant decrease in removal efficiency was reported after 5 repeated runs. The excellent  
 587 removal efficiencies of these composite materials were attributed to different reasons. An  
 588 important one is the type II heterojunction between  $g-C_3N_4$  and iron-based oxide that enhances  
 589 the charge carrier separation and transport. Another reason is the scavenging of  
 590 photogenerated electron by the adsorbent, thus increasing the charge carrier lifetime, while  
 591 the adsorbent is providing active sites for degradation reactions. Also, the presence of Fenton-  
 592 active elements (like Fe and Mn) in the composite materials can efficiently catalyze Fenton  
 593 based reactions (including photo-Fenton) for the activation of persulfate and  $H_2O_2$  into  
 594 inorganic radicals ( $HO\cdot$  and  $SO_4^{\cdot-}$ ) which are highly reactive species for the efficient destruction  
 595 of pharmaceutical compounds [80, 81].



596  
 597 **Figure 10:** Mechanism for antibiotics degradation in the magnetic  $g-C_3N_4$ - $MnFe_2O_4$ -  
 598 graphene/persulfate/vis photo-Fenton system. This figure is reproduced with permission from  
 599 Ref. [80].  
 600

601  
602

**Table 2:** Summaries of the studies reporting the integration of adsorption and photo-Fenton oxidation to remove pharmaceuticals in aqueous solutions. Studies are arranged chronologically.

Tested material	Pollutant	Experimental conditions	Removal efficiency	Ref.
Fe(II)/meso-Al <sub>2</sub> O <sub>3</sub>	Phenol (100 mg L <sup>-1</sup> )	Material = 1 g L <sup>-1</sup> ; pH = 3; t = 60 min; hv = UV; [H <sub>2</sub> O <sub>2</sub> ] = 1 μM	100%	[78]
NaX nanozeolites and CoFe <sub>2</sub> O <sub>4</sub> nanoparticles	Paracetamol and phenol (20 mg L <sup>-1</sup> each)	Material = 0.4 g L <sup>-1</sup> , pH = 3 time = 30min, hv = UVA, [H <sub>2</sub> O <sub>2</sub> ] = 50 mM	99% for both pollutants	[76, 77]
Fe <sub>3</sub> O <sub>4</sub> /coffee residue	Phenol (100 mg L <sup>-1</sup> )	Material = 1 g L <sup>-1</sup> , pH = 5, time = 120 min, hv = solar, [H <sub>2</sub> O <sub>2</sub> ] = 1.2 g L <sup>-1</sup>	100%	[72]
Fe <sub>3</sub> O <sub>4</sub> @activated carbon	Tetracycline (43 mg L <sup>-1</sup> )	Material = 0.11 g L <sup>-1</sup> , pH = 3, time = 44 min, hv = UV, [H <sub>2</sub> O <sub>2</sub> ] = 1.9 mM	79%	[82]
Fe <sub>3</sub> O <sub>4</sub> /graphene oxide nano-composite	Phenol (20 mg L <sup>-1</sup> )	Material = 0.25 g L <sup>-1</sup> , pH = 5, time = 120 min, hv = UV	98%	[83]
C <sub>3</sub> N <sub>4</sub> @MnFe <sub>2</sub> O <sub>4</sub> -graphene nanocomposites	Metronidazole (20 mg L <sup>-1</sup> )	Material = 1 g L <sup>-1</sup> , time = 90 min, hv = visible, [S <sub>2</sub> O <sub>8</sub> <sup>2-</sup> ] = 10 mM	94.5%	[80]
Fe <sub>3</sub> O <sub>4</sub> @ carbon shell	Tetracycline (60 mg L <sup>-1</sup> )	Material = 0.2 g L <sup>-1</sup> , time = 10 min, pH = 3, hv = solar, [H <sub>2</sub> O <sub>2</sub> ] = 0.55 M	100%	[84]
Activated carbon and soluble Fe(II)	7 Antibiotics: Ampicillin, clarithromycin, erythromycin, ofloxacin, sulfamethoxazole, tetracycline and trimethoprim (0.1 mg L <sup>-1</sup> each)	Material = 500 mg L <sup>-1</sup> , pH = 2.8, time = 180 min, hv = solar, [H <sub>2</sub> O <sub>2</sub> ] = 100 mg L <sup>-1</sup> , Fe(II) = 5 mg L <sup>-1</sup>	100% for all	[14]
Fe <sub>3</sub> O <sub>4</sub> / reduced graphene oxide composite	Carbamazepine (not reported)	Material = 1g L <sup>-1</sup> , pH = 6.5, time = 180 min, hv = solar	98%	[85]
LaFeO <sub>3</sub> nanoparticl deposited on Diaion <sup>TM</sup> HP21 resin	Tetracycline (10 mg L <sup>-1</sup> )	Material = 0.2 g L <sup>-1</sup> , pH = 5.7, time = 180 min, hv = visible, [H <sub>2</sub> O <sub>2</sub> ] = 10 mM	90%	[86]
Graphene oxide-magnetic nanocomposite	Caffeine	pH = 3.0 ± 0.1; H <sub>2</sub> O <sub>2</sub> = 5 mmol L <sup>-1</sup> ; catalyst = 0.2 g L <sup>-1</sup> ; caffeine = 1 mg L <sup>-1</sup> ; UV-LED (370 nm)	68% by adsorption while 98% removal by integrated treatment	[87]
Activated carbon and soluble Fe(II)	9 pharmaceuticals Chloramphenicol, fluconazole, flutamide, furosemide, gemfibrozil, ibuprofen, losartan,	Material = 0.7 g L <sup>-1</sup> , pH = 4, time = 30 min, hv = solar , [H <sub>2</sub> O <sub>2</sub> ] = 50 mg L <sup>-1</sup> , Fe(II) = 5 mg L <sup>-1</sup>	80% for fluconazole and 98-99% for the remaining 8 target pollutants	[13, 88]

	nimesulide, paracetamol (0.5 mg L <sup>-1</sup> each)			
gC <sub>3</sub> N <sub>4</sub> /Fe <sub>2</sub> O <sub>3</sub> hybrids	Tetracycline (20 mg L <sup>-1</sup> )	Material = 0.2 g L <sup>-1</sup> , time = 60 min, hv = visible, [H <sub>2</sub> O <sub>2</sub> ] = 50 mM	87%	[81]
	Amoxicillin (20 mg L <sup>-1</sup> )		62%	
	Tetracycline (20 mg L <sup>-1</sup> )		91.5%	
	Ciprofloxacin (10 mg L <sup>-1</sup> )		84%	
MoS <sub>2</sub> /FeVO <sub>4</sub> nanorods composites	Tetracycline (50 mg L <sup>-1</sup> )	Material = 1 g L <sup>-1</sup> , time = 120 min, hv = visible, [H <sub>2</sub> O <sub>2</sub> ] = 0.1 M	74%	[89]
MoS <sub>2</sub> @Schwertmannite	Roxarsone (10 mg L <sup>-1</sup> )	Material = 1 g L <sup>-1</sup> , pH = 7, time = 40 min, hv = UV, [H <sub>2</sub> O <sub>2</sub> ] = 8.8 mM	85%	[90]
FeMo <sub>3</sub> O <sub>x</sub> /g-C <sub>3</sub> N <sub>4</sub> /expanded perlite	Tetracycline (25 mg L <sup>-1</sup> )	Material = 1.33 g L <sup>-1</sup> , time = 120 min, pH = 5, hv = visible, [H <sub>2</sub> O <sub>2</sub> ] = 20 mmol <sup>-1</sup>	98%	[91]
	Oxytetracycline (25 mg L <sup>-1</sup> )		93%	
	Chlortetracycline (25 mg L <sup>-1</sup> )		97%	
Electrospun CuS nanoparticles/chitosan nanofiber composites	Tetracycline (10 mg L <sup>-1</sup> )	Material = 0.5 g L <sup>-1</sup> , time = 30 min, hv = near infrared, Material/H <sub>2</sub> O <sub>2</sub> = 0.25 wt%	65%	[92]

603

604

#### 605 4.4. Iron-based materials combined with MoS<sub>2</sub>

606 Other promising materials are those composed of MoS<sub>2</sub> and an iron-based compound. Beside  
607 the activation of photocatalysis and photo-Fenton process, MoS<sub>2</sub> has a layered structure that  
608 can play a crucial role in organic pollutant adsorption [93]. For instance, Li et al. [93]  
609 investigated magnetic Fe<sub>3</sub>O<sub>4</sub>/Fe<sub>1-x</sub>S@MoS<sub>2</sub> which can efficiently degrade tetracycline in water  
610 in the presence of H<sub>2</sub>O<sub>2</sub> Under visible light. The advantage of such a composite is its stability,  
611 high adsorption capacity and magnetic properties (thus being advantageous for post-  
612 treatment separation). However, all the processes including adsorption, photocatalysis and  
613 Fenton-based processes are discussed separately, so it is difficult to describe the contribution  
614 of each process. Other composites based on MoS<sub>2</sub> have also been investigated for the  
615 removal of pharmaceuticals. Liu et al. prepared a MoS<sub>2</sub>/FeVO<sub>4</sub> composite that can degrade  
616 70% of tetracycline after 1 h reaction under visible light in the presence of H<sub>2</sub>O<sub>2</sub> [94]. In  
617 addition, after 4 cycles, the degradation efficiency using MoS<sub>2</sub>/FeVO<sub>4</sub> composite is  
618 maintained, thus highlighting its stability. Since the photolysis of H<sub>2</sub>O<sub>2</sub> is negligible under  
619 visible light, the high degradation extent is due to integrated adsorption with both photo-Fenton  
620 and photocatalysis. Indeed, MoS<sub>2</sub> photocatalyst has excellent adsorption properties due to its  
621 layered structure. In addition, its combination with FeVO<sub>4</sub>, another photocatalyst, leads to the  
622 formation of a type II heterojunction where the photogenerated  $e^-/h^+$  pairs are efficiently  
623 separated, thus producing more reactive oxygen species (including HO<sup>•</sup> radicals).  
624 Furthermore, FeVO<sub>4</sub> contains iron which triggers Fenton-based processes. It is worth  
625 reminding that the iron cycle, especially the regeneration of Fe(II), is the limiting step in Fenton  
626 process. In MoS<sub>2</sub>/FeVO<sub>4</sub>, the reduction of Fe(III) into Fe(II) is supported by the photogenerated  
627 electrons accumulated in FeVO<sub>4</sub> and the photo-Fenton reaction (also called iron photolysis).  
628 *Wang et al.* investigated the efficiency of a composite material of MoS<sub>2</sub> and schwertmannite,  
629 an iron based mineral Fe<sub>8</sub>O<sub>8</sub>(OH)<sub>8-2x</sub>(SO<sub>4</sub>)<sub>x</sub> [90]. Schwertmannite has already shown good  
630 potential in environmental remediation via adsorption or Fenton-based oxidation processes  
631 [95-97]. Therefore, its combination with MoS<sub>2</sub> photocatalyst has been proposed as an efficient  
632 strategy for the removal of pharmaceutical compounds. Indeed, MoS<sub>2</sub>/schwertmannite can



633 efficiently remove (85% removal) roxarsone by integrated adsorption with photo-  
634 Fenton/photocatalysis in the presence of H<sub>2</sub>O<sub>2</sub> after 40 min UVA irradiation [90]. This high  
635 removal extent has been linked to the efficient iron cycling between Fe(II)/Fe(III). Indeed,  
636 similar to MoS<sub>2</sub>/FeVO<sub>4</sub>, the photogenerated electrons in MoS<sub>2</sub> can get transferred in the  
637 schwertmannite, thus subsequently reducing Fe(III) into Fe(II), while the iron photolysis under  
638 UVA light is also a factor which helps the generation of Fe(II) from Fe(III). In addition, at the  
639 composite heterojunction, Fe-O-Mo bond leads also to the reduction of Fe<sup>3+</sup> by Mo<sup>4+</sup> [90].  
640 *Wang et al.* also highlighted the important role of photogenerated holes along with the attack  
641 by hydroxyl radicals in the degradation mechanism of roxarsone [90].

642

#### 643 **4.5. Magnetic composites and other sophisticated iron-based materials**

644 Beside the integrated adsorption with photo-Fenton/photocatalysis, some issues related to  
645 post-treatment separation which limits the application of such composite materials. A  
646 promising solution is the combination of adsorbent with magnetite (Fe<sub>3</sub>O<sub>4</sub>) [84]. In addition,  
647 Fe<sub>3</sub>O<sub>4</sub> is an excellent heterogeneous photo-Fenton catalyst due to the presence of both iron(II)  
648 and iron(III), thus being an advantage for the degradation of pharmaceutical compounds in  
649 wastewater. Composites based on Fe<sub>3</sub>O<sub>4</sub> nanoparticles and carbon-based materials exhibit  
650 high specific surface area and can adsorb about 3 time more pollutants than pristine Fe<sub>3</sub>O<sub>4</sub>  
651 [82, 84, 85]. Therefore, in presence of H<sub>2</sub>O<sub>2</sub> under solar-like light, a composite based on  
652 magnetite modified by thin carbon shell (Fe<sub>3</sub>O<sub>4</sub>@HCS) can completely degrade tetracycline  
653 after 10 min reaction time [84]. Such a composite is stable since a small decrease in  
654 degradation efficiency by about 10% is observed after 5 cycles [84]. Fe<sub>3</sub>O<sub>4</sub> nanoparticles can  
655 be also immobilized on graphene oxide (Fe<sub>3</sub>O<sub>4</sub>@GO) to trigger integrated adsorption with  
656 photo-Fenton process [83]. Such composite can degrade efficiently phenol which is an  
657 important precursor for the synthesis of pharmaceutical compounds [83]. Although  
658 Fe<sub>3</sub>O<sub>4</sub>@GO has a lower adsorption capacity than pristine graphene oxide, 80% of phenol can  
659 be adsorbed after 2 hours at pH = 5 in the dark while under UV irradiation, the removal extent  
660 increases to 98% (from which 80% is fully mineralized) in the presence of H<sub>2</sub>O<sub>2</sub>. Compared to

661 pristine  $\text{Fe}_3\text{O}_4$ ,  $\text{Fe}_3\text{O}_4@\text{GO}$  enhances the degradation of phenol by about 30% thank to the  
662 integrated adsorption with photo-Fenton process, thus demonstrating the effectiveness of the  
663 bifunctional material [83]. It is worth noting  $\text{Fe}_3\text{O}_4@\text{GO}$  is also a stable composite with good  
664 reproducibility of the results after 3 successive runs while iron leaching do not exceed 0.3 mg  
665  $\text{L}^{-1}$  [83]. Similarly, reduced graphene oxide (rGO) loaded  $\text{Fe}_3\text{O}_4$  particles can degrade almost  
666 completely carbamazepine (>98%) after 3 h sunlight irradiation. The contribution of adsorption  
667 process and the photocatalytic and Fenton-based processes are both about 50%, respectively  
668 [85]. Concerning the degradation mechanism, the generation of hydroxyl radicals *via* photo-  
669 Fenton process and photocatalysis using  $\text{Fe}_3\text{O}_4$  can degrade and mineralize the  
670 pharmaceutical compounds while the graphene-based adsorbents improve their removal of  
671 by  $\pi$ - $\pi$  interactions [83]. Therefore, the degradation of phenol and carbamazepine using  
672  $\text{Fe}_3\text{O}_4@\text{GO}$  and rGO/ $\text{Fe}_3\text{O}_4$  composite is ascribed to the high adsorption capacity and efficient  
673 degradation/mineralization by the hydroxyl radicals [83, 85].

674 More sophisticated magnetic materials can be also designed for the removal of  
675 pharmaceuticals [98, 99]. For instance,  $\text{FeNi}_3@\text{SiO}_2@\text{ZnO}$  can remove completely of  
676 penicillin G after 2 h UVA irradiation [99]. In such an integrated system,  $\text{FeNi}_3$  plays the role  
677 of the magnetic component for easy post-separation treatment, while  $\text{SiO}_2$  and  $\text{ZnO}$  are the  
678 adsorbent and the photocatalyst, respectively [99]. The photo-Fenton process for such a  
679 system has not been yet investigated but it appears promising. It is because a similar  
680 composite material,  $\text{FeNi}_3/\text{SiO}_2$ , has shown promising ability in coupled adsorption and  
681 Fenton-like oxidation for the degradation of metronidazole [98]. About 80% of the  
682 metronidazole was removed during this process. Reusability tests showed a slight decrease  
683 (of about 8%) in the removal efficiency from the first cycle to the sixth cycle demonstrating the  
684 strong stability of this material.

685

#### 686 **4.6. Stability of iron-based materials for integrated adsorption with photochemical** 687 **process**

688 All the above mentioned composite materials integrate adsorption with photo-Fenton process  
689 and/or photocatalysis. However, in such photoactive materials containing iron, it is well known  
690 that iron can be leached under light irradiation due to the photolysis of iron. Since most of  
691 these composite materials contain an adsorbing component (e.g. carbon-based adsorbents),  
692 this potential leaching of iron can be limited, while ternary oxide like  $\text{MnFe}_2\text{O}_4$  is highly stable,  
693 so no leaching occurs [83]. In addition, the adsorbents which are initially used for the  
694 adsorption of the target contaminants can also adsorb the degradation byproducts, thus (i)  
695 removing the remaining pollution which cannot be degrade by photo-Fenton process and (ii)  
696 supporting the photochemical reactions at the surface of the composite material [79]. Indeed,  
697 the adsorption ability of the composite, not only facilitates the interaction of the contaminant  
698 with its surface, but can also increase the transfer of photogenerated radicals leading to higher  
699 degradation extents [86]. However, the adsorption process can also affect negatively the  
700 photochemical processes where the adsorbed pharmaceuticals (and degradation byproducts)  
701 can hinder light utilization by the composite material, thus decreasing the degradation  
702 efficiency of the contaminants [86]. Nevertheless, the integrated adsorption with  
703 photocatalysis and photo-Fenton process is among the most efficient and innovative methods  
704 to efficiently remove pharmaceutical compounds thank to the bifunctionality of such composite  
705 materials. Therefore, integrated adsorption with photo-Fenton and photocatalysis is highly  
706 relevant for efficient decontamination of wastewaters.

707

#### 708 **5. Conclusions and outlooks**

709 The use of dual-functional materials to develop integrated treatments based on Fenton  
710 oxidation and adsorption could be a highly efficient and cost-effective water treatment.  
711 However, it is essential to overcome significant challenges before bench-scale findings can  
712 be translated to field applications. Some of these challenges are associated to the treatment

713 process while others are inherent to the tested materials (heterogeneous catalysts and  
714 adsorbents) that pose challenges to treatment system. A brief description of major findings is  
715 provided below:

- 716 • The development of cost-effective and efficient materials for this purpose is a  
717 promising field. It would be highly rewarding to develop materials which are multi-  
718 functional, efficient, environment-friendly, stable, and reusable. Innovative materials  
719 can broaden the utility of their applications. Magnetic nanomaterials and  
720 nanoarchitectures are showing great potential but their practical feasibility,  
721 environmental fate, and stability remains questionable. Magnetic materials when  
722 exposed to air can develop a passivating layer on its surface that affects the redox  
723 reactivity, a phenomenon that turn out to be predominantly significant for nanosized  
724 particles with a higher surface-to-volume ratio [20]. Therefore, finding suitable  
725 strategies to further improve the stability and efficiency of these materials (e.g.  
726 appropriate coating, composites) is needed. In addition to these solid treatments, the  
727 addition of other reagents during the reaction may also improve the treatment  
728 efficiency. For example, our recent study showed that the application of ascorbic acid,  
729 an environment-friendly reducing agent, improved the magnetite-mediated Fenton  
730 oxidation for higher removal of pentachlorophenol [100]. The reducing capacity of  
731 ascorbic acid enabled the magnetite to maintain its structural Fe(II) contents during the  
732 oxidation reaction.
- 733 • The development of bioinspired materials has also been suggested as a suitable  
734 alternative to the chemically-synthesized supports but better understanding of their  
735 stability and efficiency is required in wastewater. Further investigations are certainly  
736 needed in order to optimize the operational parameters for high-scale production of  
737 bioinspired materials.
- 738 • Further integration of these processes with biological treatments should also be sought  
739 to make them environmentally attractive. This, however, remains a challenge due to  
740 drastic impacts of chemical oxidants on microbial/biota activity which should be

741 addressed. The chances of improvement exist in preparing the environment-friendly  
742 reusable materials, improving the treatment efficiency, and reducing the quantities of  
743 chemical oxidants.

744 • Another critical issue in research focused on hybrid treatments is the laboratory scale  
745 investigations. Many studies rely on artificially-contaminated water containing only the  
746 target pollutant and often at much higher concentrations. In real systems, however,  
747 natural organic matter is found in much higher amounts than target pollutants which  
748 would decrease the oxidation efficiency due to non-target consumption of materials  
749 and oxidants [10]. Thus, these hybrid treatments could suffer from reduced  
750 performance in complex water matrices. For this, more studies are needed on real  
751 water/wastewater representative samples to identify the materials with better potential  
752 for field scale applications. Moreover, the quality and quantity of contaminated water  
753 dictate the choice of appropriate material/treatment. Hence, a thorough site-specific  
754 characterization of water is needed prior to their treatment.

755 • Non-selective nature of adsorption can become a potential drawback in aqueous  
756 systems contaminated with a variety of pollutants. To address this, the development  
757 of adsorbents with preferential adsorption properties could be advantageous. It will  
758 likely concentrate the target pollutants for an ex-situ Fenton oxidation treatment.  
759 Moreover, sequential treatment cycles of adsorption and oxidation processes in  
760 separate reactors/tanks could also be considered as a means to overcome drawbacks  
761 caused by the multi-contamination of real wastewaters. Finally, efforts should be made  
762 to upscale the findings to simulated realistic conditions and real field applications.

763 • Despite success in laboratory, the translation of hybrid treatments for field application  
764 remains at an early stage of development. Future research should focus on rationally  
765 designing the dual-functional materials for their intended use.

766 • Finally, an accurate assessment of the value of dual-functional materials with respect  
767 to cost and life-cycle impacts is crucial for the successful implementation of these  
768 materials.

769  
770 **Acknowledgments**

771 M. Usman, B. Hameed and M. Al-Abri acknowledge the joint support by Qatar University,  
772 Qatar and Sultan Qaboos University, Oman, under the international research collaboration  
773 grant (IRCC-2021-014; CL/SQU-QU/CESR/21/01). O. Monfort and S. Gowrisankaran  
774 acknowledge the support of the Slovak Research and Development Agency (project APVV-  
775 21-0039) and the European Regional Fund within the Operational Programme Integrated  
776 Infrastructure (project USCCCOR – ZoNFP: NFP313020BUZ3). The findings achieved  
777 herein are solely the responsibility of the authors.

778

779 **Conflict of Interest**

780 The authors declare no conflict of interest.

781

- 784 [1] M. Patel, R. Kumar, K. Kishor, T. Mlsna, C.U. Pittman, D. Mohan, Pharmaceuticals of  
785 emerging concern in aquatic systems: Chemistry, occurrence, effects, and removal  
786 methods, *Chem. Rev.*, 119 (2019) 3510-3673.
- 787 [2] J. Rivera-Utrilla, M. Sánchez-Polo, M.Á. Ferro-García, G. Prados-Joya, R. Ocampo-  
788 Pérez, Pharmaceuticals as emerging contaminants and their removal from water. A review,  
789 *Chemosphere*, 93 (2013) 1268-1287.
- 790 [3] A. Ginebreda, I. Muñoz, M.L. de Alda, R. Brix, J. López-Doval, D. Barceló, Environmental  
791 risk assessment of pharmaceuticals in rivers: Relationships between hazard indexes and  
792 aquatic macroinvertebrate diversity indexes in the Llobregat River (NE Spain), *Environment*  
793 *International*, 36 (2010) 153-162.
- 794 [4] H. The Lancet Planetary, The natural environment and emergence of antibiotic  
795 resistance, *The Lancet Planetary Health*, 2 (2018) e1.
- 796 [5] US Centre for Disease Prevention and Control. Measuring Outpatient Antibiotic  
797 Prescribing, 2019.
- 798 [6] M. Usman, M. Farooq, K. Hanna, Environmental side effects of the injudicious use of  
799 antimicrobials in the era of COVID-19, *Sci. Total Environ.*, 745 (2020) 141053.
- 800 [7] K. Kümmerer, D.D. Dionysiou, O. Olsson, D. Fatta-Kassinos, A path to clean water,  
801 *Science*, 361 (2018) 222.
- 802 [8] M. Usman, S. Martin, N. Cimetière, S. Giraudet, V. Chatain, K. Hanna, Sorption of  
803 Nalidixic Acid onto Micrometric and Nanometric Magnetites: Experimental Study and  
804 Modeling, *Appl. Surf. Sci.*, 299C (2014) 136-145.
- 805 [9] M. Jain, A. Mudhoo, D.L. Ramasamy, M. Najafi, M. Usman, R. Zhu, G. Kumar, S.  
806 Shobana, V.K. Garg, M. Sillanpää, Adsorption, degradation, and mineralization of emerging  
807 pollutants (pharmaceuticals and agrochemicals) by nanostructures: a comprehensive  
808 review, *Environ Sci Pollut Res*, 27 (2020) 34862-34905.
- 809 [10] B.C. Hodges, E.L. Cates, J.-H. Kim, Challenges and prospects of advanced oxidation  
810 water treatment processes using catalytic nanomaterials, *Nature Nanotechnology*, 13 (2018)  
811 642-650.
- 812 [11] M. Usman, Y.-S. Ho, A bibliometric study of the Fenton oxidation for soil and water  
813 remediation, *J. Environ. Manage.*, 270 (2020) 110886.
- 814 [12] A.-Y. Zhang, N.-H. Huang, C. Zhang, P.-C. Zhao, T. Lin, Y.-Y. He, J.-W. Feng,  
815 Heterogeneous Fenton decontamination of organoarsenicals and simultaneous adsorption  
816 of released arsenic with reduced secondary pollution, *Chem. Eng. J.*, 344 (2018) 1-11.
- 817 [13] A. Della-Flora, M.L. Wilde, P.S. Thue, D. Lima, E.C. Lima, C. Sirtori, Combination of  
818 solar photo-Fenton and adsorption process for removal of the anticancer drug Flutamide and  
819 its transformation products from hospital wastewater, *J. Hazard. Mater.*, 396 (2020) 122699.
- 820 [14] S.G. Michael, I. Michael-Kordatou, V.G. Beretsou, T. Jäger, C. Michael, T. Schwartz, D.  
821 Fatta-Kassinos, Solar photo-Fenton oxidation followed by adsorption on activated carbon for  
822 the minimisation of antibiotic resistance determinants and toxicity present in urban  
823 wastewater, *Applied Catalysis B: Environmental*, 244 (2019) 871-880.
- 824 [15] A. Kumar, A. Rana, G. Sharma, M. Naushad, P. Dhiman, A. Kumari, F.J. Stadler,  
825 Recent advances in nano-Fenton catalytic degradation of emerging pharmaceutical  
826 contaminants, *J. Mol. Liq.*, 290 (2019) 111177.
- 827 [16] M. Bilal, K. Rizwan, M. Adeel, H.M.N. Iqbal, Hydrogen-based catalyst-assisted  
828 advanced oxidation processes to mitigate emerging pharmaceutical contaminants, *Int. J.*  
829 *Hydrogen Energy*, 47 (2022) 19555-19569.
- 830 [17] I. Ihsanullah, M.T. Khan, M. Zubair, M. Bilal, M. Sajid, Removal of pharmaceuticals from  
831 water using sewage sludge-derived biochar: A review, *Chemosphere*, 289 (2022) 133196.
- 832 [18] E.D.V. Duarte, M.G. Oliveira, M.P. Spaolonzi, H.P.S. Costa, T.L.d. Silva, M.G.C.d. Silva,  
833 M.G.A. Vieira, Adsorption of pharmaceutical products from aqueous solutions on  
834 functionalized carbon nanotubes by conventional and green methods: A critical review,  
835 *Journal of Cleaner Production*, 372 (2022) 133743.

836 [19] M. Usman, S. Jellali, I. Anastopoulos, Y. Charabi, B.H. Hameed, K. Hanna, Fenton  
837 oxidation for soil remediation: A critical review of observations in historically contaminated  
838 soils, *J. Hazard. Mater.*, 424 (2022) 127670.

839 [20] M. Usman, J.M. Byrne, A. Chaudhary, S. Orsetti, K. Hanna, C. Ruby, A. Kappler, S.B.  
840 Haderlein, Magnetite and Green Rust: Synthesis, Properties, and Environmental  
841 Applications of Mixed-Valent Iron Minerals, *Chem. Rev.*, 118 (2018) 3251-3304.

842 [21] S. Zha, Y. Cheng, Y. Gao, Z. Chen, M. Megharaj, R. Naidu, Nanoscale zero-valent iron  
843 as a catalyst for heterogeneous Fenton oxidation of amoxicillin, *Chem. Eng. J.*, 255 (2014)  
844 141-148.

845 [22] Y. Zhang, L. Zhao, Y. Yang, P. Sun, Fenton-Like Oxidation of Antibiotic Ornidazole  
846 Using Biochar-Supported Nanoscale Zero-Valent Iron as Heterogeneous Hydrogen Peroxide  
847 Activator, *International Journal of Environmental Research and Public Health*, 17 (2020)  
848 1324.

849 [23] A. Liu, J. Liu, J. Han, W.-x. Zhang, Evolution of nanoscale zero-valent iron (nZVI) in  
850 water: Microscopic and spectroscopic evidence on the formation of nano- and micro-  
851 structured iron oxides, *J. Hazard. Mater.*, 322 (2017) 129-135.

852 [24] M.L. Tran, C.H. Nguyen, T.T.V. Tran, R.-S. Juang, One-pot synthesis of bimetallic  
853 Pt/nZVI nanocomposites for enhanced removal of oxytetracycline: Roles of morphology  
854 changes and Pt catalysis, *Journal of the Taiwan Institute of Chemical Engineers*, 111 (2020)  
855 130-140.

856 [25] S. Bae, R.N. Collins, T.D. Waite, K. Hanna, Advances in Surface Passivation of  
857 Nanoscale Zerovalent Iron: A Critical Review, *Environ. Sci. Technol.*, 52 (2018) 12010-  
858 12025.

859 [26] X. Weng, G. Owens, Z. Chen, Synergetic adsorption and Fenton-like oxidation for  
860 simultaneous removal of ofloxacin and enrofloxacin using green synthesized Fe NPs, *Chem.*  
861 *Eng. J.*, 382 (2020) 122871.

862 [27] L. Chen, R. Ni, T. Yuan, Y. Gao, W. Kong, P. Zhang, Q. Yue, B. Gao, Effects of green  
863 synthesis, magnetization, and regeneration on ciprofloxacin removal by bimetallic nZVI/Cu  
864 composites and insights of degradation mechanism, *J. Hazard. Mater.*, 382 (2020) 121008.

865 [28] A. Masud, N.G. Chavez Soria, D.S. Aga, N. Aich, Adsorption and advanced oxidation of  
866 diverse pharmaceuticals and personal care products (PPCPs) from water using highly  
867 efficient rGO-nZVI nanohybrids, *Environmental Science: Water Research & Technology*, 6  
868 (2020) 2223-2238.

869 [29] Z. Wan, J. Wang, Ce-Fe-reduced graphene oxide nanocomposite as an efficient  
870 catalyst for sulfamethazine degradation in aqueous solution, *Environ Sci Pollut Res*, 23  
871 (2016) 18542-18551.

872 [30] Y. Yang, L. Xu, W. Li, W. Fan, S. Song, J. Yang, Adsorption and degradation of  
873 sulfadiazine over nanoscale zero-valent iron encapsulated in three-dimensional graphene  
874 network through oxygen-driven heterogeneous Fenton-like reactions, *Applied Catalysis B:*  
875 *Environmental*, 259 (2019) 118057.

876 [31] C.H. Nguyen, M.L. Tran, T.T. Van Tran, R.-S. Juang, Efficient removal of antibiotic  
877 oxytetracycline from water by Fenton-like reactions using reduced graphene oxide-  
878 supported bimetallic Pd/nZVI nanocomposites, *Journal of the Taiwan Institute of Chemical*  
879 *Engineers*, 119 (2021) 80-89.

880 [32] L. Chen, T. Yuan, R. Ni, Q. Yue, B. Gao, Multivariate optimization of ciprofloxacin  
881 removal by polyvinylpyrrolidone stabilized NZVI/Cu bimetallic particles, *Chem. Eng. J.*, 365  
882 (2019) 183-192.

883 [33] N.S. Shah, J.A. Khan, M. Sayed, J. Iqbal, Z.U.H. Khan, N. Muhammad, K.  
884 Polychronopoulou, S. Hussain, M. Imran, B. Murtaza, M. Usman, I. Ismail, A. Shafique, F.  
885 Howari, Y. Nazzal, Nano-zerovalent copper as a Fenton-like catalyst for the degradation of  
886 ciprofloxacin in aqueous solution, *Journal of Water Process Engineering*, 37 (2020) 101325.

887 [34] E.S. Emídio, P. Hammer, R.F.P. Nogueira, Simultaneous degradation of the anticancer  
888 drugs 5-fluorouracil and cyclophosphamide using a heterogeneous photo-Fenton process  
889 based on copper-containing magnetites (Fe<sub>3</sub>-xCu<sub>x</sub>O<sub>4</sub>), *Chemosphere*, 241 (2020) 124990.



890 [35] N. Zhang, J. Chen, Z. Fang, E.P. Tsang, Ceria accelerated nanoscale zerovalent iron  
891 assisted heterogenous Fenton oxidation of tetracycline, *Chem. Eng. J.*, 369 (2019) 588-599.

892 [36] J. Tang, J. Wang, MOF-derived three-dimensional flower-like FeCu@C composite as an  
893 efficient Fenton-like catalyst for sulfamethazine degradation, *Chem. Eng. J.*, 375 (2019)  
894 122007.

895 [37] R.M. Cornell, U. Schwertmann, *The Iron Oxides: Structure, Properties, Reactions,*  
896 *Occurrence and Uses*, Second ed., Wiley-VCH2003.

897 [38] A. Hassani, M. Karaca, S. Karaca, A. Khataee, Ö. Açışlı, B. Yılmaz, Preparation of  
898 magnetite nanoparticles by high-energy planetary ball mill and its application for  
899 ciprofloxacin degradation through heterogeneous Fenton process, *Journal of Environmental*  
900 *Management*, 211 (2018) 53-62.

901 [39] N. Sharifi, A. Nasiri, S. Silva Martínez, H. Amiri, Synthesis of Fe<sub>3</sub>O<sub>4</sub>@activated carbon  
902 to treat metronidazole effluents by adsorption and heterogeneous Fenton with effluent  
903 bioassay, *Journal of Photochemistry and Photobiology A: Chemistry*, 427 (2022) 113845.

904 [40] D. Shan, S. Deng, C. Jiang, Y. Chen, B. Wang, Y. Wang, J. Huang, G. Yu, M.R.  
905 Wiesner, Hydrophilic and strengthened 3D reduced graphene oxide/nano-Fe<sub>3</sub>O<sub>4</sub> hybrid  
906 hydrogel for enhanced adsorption and catalytic oxidation of typical pharmaceuticals,  
907 *Environmental Science: Nano*, 5 (2018) 1650-1660.

908 [41] Y. Liu, N. Tan, B. Wang, Y. Liu, Stepwise adsorption-oxidation removal of  
909 oxytetracycline by ZnO-CNTs-Fe<sub>3</sub>O<sub>4</sub> from aqueous solution, *Chem. Eng. J.*, 375 (2019)  
910 121963.

911 [42] K.V. Plakas, A. Mantza, S.D. Sklari, V.T. Zaspalis, A.J. Karabelas, Heterogeneous  
912 Fenton-like oxidation of pharmaceutical diclofenac by a catalytic iron-oxide ceramic  
913 microfiltration membrane, *Chem. Eng. J.*, 373 (2019) 700-708.

914 [43] W. Huang, F. Wang, N. Qiu, X. Wu, C. Zang, A. Li, L. Xu, Enteromorpha prolifera-  
915 derived Fe<sub>3</sub>C/C composite as advanced catalyst for hydroxyl radical generation and efficient  
916 removal for organic dye and antibiotic, *J. Hazard. Mater.*, 378 (2019) 120728.

917 [44] N. Nasseh, L. Taghavi, B. Barikbin, M.A. Nasser, A. Allahresani, FeNi<sub>3</sub>/SiO<sub>2</sub> magnetic  
918 nanocomposite as an efficient and recyclable heterogeneous fenton-like catalyst for the  
919 oxidation of metronidazole in neutral environments: Adsorption and degradation studies,  
920 *Composites Part B: Engineering*, 166 (2019) 328-340.

921 [45] G. Wang, D. Zhao, F. Kou, Q. Ouyang, J. Chen, Z. Fang, Removal of norfloxacin by  
922 surface Fenton system (MnFe<sub>2</sub>O<sub>4</sub>/H<sub>2</sub>O<sub>2</sub>): Kinetics, mechanism and degradation pathway,  
923 *Chem. Eng. J.*, 351 (2018) 747-755.

924 [46] B. Bai, X. Xu, C. Li, J. Xing, H. Wang, Y. Suo, Magnetic Fe<sub>3</sub>O<sub>4</sub>@Chitosan Carbon  
925 Microbeads: Removal of Doxycycline from Aqueous Solutions through a Fixed Bed via  
926 Sequential Adsorption and Heterogeneous Fenton-Like Regeneration, *Journal of*  
927 *Nanomaterials*, 2018 (2018) 5296410.

928 [47] M. Usman, O. Tascone, V. Rybnikova, P. Faure, K. Hanna, Application of chemical  
929 oxidation to remediate HCH-contaminated soil under batch and flow through conditions,  
930 *Environ Sci Pollut Res*, 24 (2017) 14748-14757.

931 [48] J. Ma, M. Yang, F. Yu, J. Chen, Easy solid-phase synthesis of pH-insensitive  
932 heterogeneous CNTs/FeS Fenton-like catalyst for the removal of antibiotics from aqueous  
933 solution, *J. Colloid Interface Sci.*, 444 (2015) 24-32.

934 [49] Y. Liu, X. Zhang, J. Deng, Y. Liu, A novel CNTs-Fe<sub>3</sub>O<sub>4</sub> synthesized via a ball-milling  
935 strategy as efficient fenton-like catalyst for degradation of sulfonamides, *Chemosphere*, 277  
936 (2021) 130305.

937 [50] J. Li, L. Pan, G. Yu, S. Xie, C. Li, D. Lai, Z. Li, F. You, Y. Wang, The synthesis of  
938 heterogeneous Fenton-like catalyst using sewage sludge biochar and its application for  
939 ciprofloxacin degradation, *Sci. Total Environ.*, 654 (2019) 1284-1292.

940 [51] Y. Yu, F. Huang, Y. He, X. Liu, C. Song, Y. Xu, Y. Zhang, Heterogeneous fenton-like  
941 degradation of ofloxacin over sludge derived carbon as catalysts: Mechanism and  
942 performance, *Sci. Total Environ.*, 654 (2019) 942-947.

943 [52] M. Haris, Y. Hamid, M. Usman, L. Wang, A. Saleem, F. Su, J. Guo, Y. Li, Crop-residues  
944 derived biochar: Synthesis, properties, characterization and application for the removal of  
945 trace elements in soils, *J. Hazard. Mater.*, 416 (2021) 126212.

946 [53] S. Jellali, B. Khiari, M. Usman, H. Hamdi, Y. Charabi, M. Jeguirim, Sludge-derived  
947 biochars: A review on the influence of synthesis conditions on pollutants removal efficiency  
948 from wastewaters, *Renew. Sust. Energ. Rev.*, 144 (2021) 111068.

949 [54] Y. Xie, X. Wang, W. Tong, W. Hu, P. Li, L. Dai, Y. Wang, Y. Zhang, FexP/biochar  
950 composites induced oxygen-driven Fenton-like reaction for sulfamethoxazole removal:  
951 Performance and reaction mechanism, *Chem. Eng. J.*, 396 (2020) 125321.

952 [55] W. Gu, X. Huang, Y. Tian, M. Cao, L. Zhou, Y. Zhou, J. Lu, J. Lei, Y. Zhou, L. Wang, Y.  
953 Liu, J. Zhang, High-efficiency adsorption of tetracycline by cooperation of carbon and iron in  
954 a magnetic Fe/porous carbon hybrid with effective Fenton regeneration, *Appl. Surf. Sci.*, 538  
955 (2021) 147813.

956 [56] S. Zhuang, J. Wang, Magnetic COFs as catalyst for Fenton-like degradation of  
957 sulfamethazine, *Chemosphere*, 264 (2021) 128561.

958 [57] A.S. Mutia, T. Ariyanto, I. Prasetyo, Ciprofloxacin Removal from Simulated Wastewater  
959 Through a Combined Process of Adsorption and Oxidation Processes Using Fe/C  
960 Adsorbent, *Water, Air, & Soil Pollution*, 233 (2022) 146.

961 [58] H. Ma, B. Yu, Q. Wang, G. Owens, Z. Chen, Enhanced removal of pefloxacin from  
962 aqueous solution by adsorption and Fenton-like oxidation using NH<sub>2</sub>-MIL-88B, *J. Colloid  
963 Interface Sci.*, 583 (2021) 279-287.

964 [59] Y. Liu, J. Li, L. Wu, D. Wan, Y. Shi, Q. He, J. Chen, Synergetic adsorption and Fenton-  
965 like degradation of tetracycline hydrochloride by magnetic spent bleaching earth carbon:  
966 Insights into performance and reaction mechanism, *Sci. Total Environ.*, 761 (2021) 143956.

967 [60] H. Titouhi, J.-E. Belgaied, Heterogeneous Fenton oxidation of ofloxacin drug by iron  
968 alginate support, *Environ. Technol.*, 37 (2016) 2003-2015.

969 [61] G. Wang, J. Xiang, J. Lin, L. Xiang, S. Chen, B. Yan, H. Fan, S. Zhang, X. Shi,  
970 Sustainable Advanced Fenton-like Catalysts Based on Mussel-Inspired Magnetic Cellulose  
971 Nanocomposites to Effectively Remove Organic Dyes and Antibiotics, *ACS Applied  
972 Materials & Interfaces*, 12 (2020) 51952-51959.

973 [62] X. Hou, J. Shi, N. Wang, Z. Wen, M. Sun, J. Qu, Q. Hu, Removal of antibiotic  
974 tetracycline by metal-organic framework MIL-101(Cr) loaded nano zero-valent iron, *J. Mol.  
975 Liq.*, 313 (2020) 113512.

976 [63] A.V. Russo, B.G. Merlo, S.E. Jacobo, Adsorption and catalytic degradation of Tartrazine  
977 in aqueous medium by a Fe-modified zeolite, *Cleaner Engineering and Technology*, 4 (2021)  
978 100211.

979 [64] C. Zhou, H. Zhou, Y. Yuan, J. Peng, G. Yao, P. Zhou, B. Lai, Coupling adsorption and  
980 in-situ Fenton-like oxidation by waste leather-derived materials in continuous flow mode  
981 towards sustainable removal of trace antibiotics, *Chem. Eng. J.*, 420 (2021) 130370.

982 [65] S. Rahimi, T. Al-Musawi, F.S. Arghavan, N. Nasseh, Mechanism and efficiency of  
983 metronidazole removal via adsorption and heterogeneous Fenton reaction using FeNi 3  
984 nanoparticles, *Desalination and Water Treatment*, 234 (2021) 136–146.

985 [66] X. Ding, Y. Liu, X. Chen, W. Liu, J. Li, Simultaneous Removal of Antibiotics and Heavy  
986 Metals with Poly(Aspartic Acid)-Based Fenton Micromotors, *Chemistry – An Asian Journal*,  
987 16 (2021) 1930-1936.

988 [67] X. Yang, C. Lai, L. Li, M. Cheng, S. Liu, H. Yi, M. Zhang, Y. Fu, F. Xu, H. Yan, X. Liu, B.  
989 Li, Oxygen vacancy assisted Mn-CuO Fenton-like oxidation of ciprofloxacin: Performance,  
990 effects of pH and mechanism, *Sep. Purif. Technol.*, 287 (2022) 120517.

991 [68] X. Song, J. Mo, Y. Fang, S. Luo, J. Xu, X. Wang, Synthesis of magnetic nanocomposite  
992 Fe<sub>3</sub>O<sub>4</sub>@ZIF-8@ZIF-67 and removal of tetracycline in water, *Environ Sci Pollut Res*, 29  
993 (2022) 35204-35216.

994 [69] X. Nie, G. Li, S. Li, Y. Luo, W. Luo, Q. Wan, T. An, Highly efficient adsorption and  
995 catalytic degradation of ciprofloxacin by a novel heterogeneous Fenton catalyst of hexapod-  
996 like pyrite nanosheets mineral clusters, *Applied Catalysis B: Environmental*, 300 (2022)  
997 120734.

998 [70] S. Rahim Pouran, A.R. Abdul Aziz, W.M.A. Wan Daud, Review on the main advances in  
999 photo-Fenton oxidation system for recalcitrant wastewaters, *Journal of Industrial and*  
1000 *Engineering Chemistry*, 21 (2015) 53-69.

1001 [71] L. Clarizia, D. Russo, I. Di Somma, R. Marotta, R. Andreozzi, Homogeneous photo-  
1002 Fenton processes at near neutral pH: A review, *Applied Catalysis B: Environmental*, 209  
1003 (2017) 358-371.

1004 [72] A.A. Oladipo, M.A. Abureesh, M. Gazi, Bifunctional composite from spent "Cyprus  
1005 coffee" for tetracycline removal and phenol degradation: Solar-Fenton process and artificial  
1006 neural network, *Int. J. Biol. Macromol.*, 90 (2016) 89-99.

1007 [73] K.A. Azalok, A.A. Oladipo, M. Gazi, Hybrid MnFe-LDO–biochar nanopowders for  
1008 degradation of metronidazole via UV-light-driven photocatalysis: Characterization and  
1009 mechanism studies, *Chemosphere*, 268 (2021) 128844.

1010 [74] F.S. Mustafa, A.A. Oladipo, Photocatalytic degradation of metronidazole and bacteria  
1011 disinfection activity of Ag–doped Ni<sub>0.5</sub>Zn<sub>0.5</sub>Fe<sub>2</sub>O<sub>4</sub>, *Journal of Water Process Engineering*,  
1012 42 (2021) 102132.

1013 [75] Y. Nosaka, A.Y. Nosaka, Generation and Detection of Reactive Oxygen Species in  
1014 Photocatalysis, *Chem. Rev.*, 117 (2017) 11302-11336.

1015 [76] M. Irani, L.R. Rad, H. Pourahmad, I. Haririan, Optimization of the combined  
1016 adsorption/photo-Fenton method for the simultaneous removal of phenol and paracetamol in  
1017 a binary system, *Microporous Mesoporous Mater.*, 206 (2015) 1-7.

1018 [77] L.R. Rad, I. Haririan, F. Divsar, Comparison of adsorption and photo-Fenton processes  
1019 for phenol and paracetamol removing from aqueous solutions: Single and binary systems,  
1020 *Spectrochimica Acta - Part A: Molecular and Biomolecular Spectroscopy*, 136 (2015) 423-  
1021 428.

1022 [78] K.M. Parida, A.C. Pradhan, Fe/meso-Al<sub>2</sub>O<sub>3</sub>: An efficient photo-fenton catalyst for the  
1023 adsorptive degradation of phenol, *Ind. Eng. Chem. Res.*, 49 (2010) 8310-8318.

1024 [79] A. Della-Flora, M.L. Wilde, D. Lima, E.C. Lima, C. Sirtori, Combination of tertiary solar  
1025 photo-Fenton and adsorption processes in the treatment of hospital wastewater: The  
1026 removal of pharmaceuticals and their transformation products, *Journal of Environmental*  
1027 *Chemical Engineering*, 9 (2021) 105666-105666.

1028 [80] X. Wang, A. Wang, J. Ma, Visible-light-driven photocatalytic removal of antibiotics by  
1029 newly designed C<sub>3</sub>N<sub>4</sub>@MnFe<sub>2</sub>O<sub>4</sub>-graphene nanocomposites, *J. Hazard. Mater.*, 336 (2017)  
1030 81-92.

1031 [81] H. Zhao, C. Tian, J. Mei, S. Yang, P.K. Wong, Faster electron injection and higher  
1032 interface reactivity in g-C<sub>3</sub>N<sub>4</sub>/Fe<sub>2</sub>O<sub>3</sub> nanohybrid for efficient photo-Fenton-like activity  
1033 toward antibiotics degradation, *Environ. Res.*, 195 (2021) 110842-110842.

1034 [82] B. Kakavandi, A. Takdastan, N. Jaafarzadeh, M. Azizi, A. Mirzaei, A. Azari, Application  
1035 of Fe<sub>3</sub>O<sub>4</sub>@C catalyzing heterogeneous UV-Fenton system for tetracycline removal with a  
1036 focus on optimization by a response surface method, *Journal of Photochemistry and*  
1037 *Photobiology A: Chemistry*, 314 (2016) 178-188.

1038 [83] L. Yu, J. Chen, Z. Liang, W. Xu, L. Chen, D. Ye, Degradation of phenol using Fe<sub>3</sub>O<sub>4</sub>-  
1039 GO nanocomposite as a heterogeneous photo-Fenton catalyst, *Sep. Purif. Technol.*, 171  
1040 (2016) 80-87.

1041 [84] X. Yan, K. Gan, B. Tian, J. Zhang, L. Wang, D. Lu, Photo-fenton refreshable  
1042 Fe<sub>3</sub>O<sub>4</sub>@HCS adsorbent for the elimination of tetracycline hydrochloride, *Res. Chem.*  
1043 *Intermed.*, 44 (2018).

1044 [85] M. Moztahida, J. Jang, M. Nawaz, S.R. Lim, D.S. Lee, Effect of rGO loading on Fe<sub>3</sub>O<sub>4</sub>  
1045 : A visible light assisted catalyst material for carbamazepine degradation, *Sci. Total*  
1046 *Environ.*, 667 (2019) 741-750.

1047 [86] A. Alpay, Ö. Tuna, E.B. Simsek, Deposition of perovskite-type LaFeO<sub>3</sub> particles on  
1048 spherical commercial polystyrene resin: A new platform for enhanced photo-Fenton-  
1049 catalyzed degradation and simultaneous wastewater purification, *Environmental Technology*  
1050 *and Innovation*, 20 (2020) 101175-101175.

1051 [87] M.A. Ramirez-Ubillus, N. de Melo Costa-Serge, P. Hammer, R.F.P. Nogueira, A new  
1052 approach on synergistic effect and chemical stability of graphene oxide-magnetic

1053 nanocomposite in the heterogeneous Fenton degradation of caffeine, *Environ Sci Pollut*  
1054 *Res*, 28 (2021) 55014-55028.

1055 [88] A. Della-Flora, M.L. Wilde, D. Lima, E.C. Lima, C. Sirtori, Combination of tertiary solar  
1056 photo-Fenton and adsorption processes in the treatment of hospital wastewater: The  
1057 removal of pharmaceuticals and their transformation products, *Journal of Environmental*  
1058 *Chemical Engineering*, 9 (2021) 105666.

1059 [89] Q. Liu, J. Zhao, Y. Wang, Y. Liu, J. Dong, J. Xia, H. Li, The novel photo-Fenton-like few-  
1060 layer MoS<sub>2</sub>/FeVO<sub>4</sub> composite for improved degradation activity under visible light  
1061 irradiation, *Colloids and Surfaces A: Physicochemical and Engineering Aspects*, 623 (2021)  
1062 126721.

1063 [90] X. Wang, Y. Chen, T. Li, J. Liang, L. Zhou, High-efficient elimination of roxarsone by  
1064 MoS<sub>2</sub>@Schwertmannite via heterogeneous photo-Fenton oxidation and simultaneous  
1065 arsenic immobilization, *Chem. Eng. J.*, 405 (2021) 126952-126952.

1066 [91] Y. Liu, X. Wang, Q. Sun, M. Yuan, Z. Sun, S. Xia, J. Zhao, Enhanced visible light photo-  
1067 Fenton-like degradation of tetracyclines by expanded perlite supported FeMo<sub>3</sub>O<sub>x</sub>/g-C<sub>3</sub>N<sub>4</sub>  
1068 floating Z-scheme catalyst, *J. Hazard. Mater.*, 424 (2022) 127387.

1069 [92] G.-Y. Huang, W.-J. Chang, T.-W. Lu, I.L. Tsai, S.-J. Wu, M.-H. Ho, F.-L. Mi, Electrospun  
1070 CuS nanoparticles/chitosan nanofiber composites for visible and near-infrared light-driven  
1071 catalytic degradation of antibiotic pollutants, *Chem. Eng. J.*, 431 (2022) 134059.

1072 [93] J. Li, X. Zhang, T. Wang, Y. Zhao, T. Song, L. Zhang, X. Cheng, Construction of layered  
1073 hollow Fe<sub>3</sub>O<sub>4</sub>/Fe<sub>1-x</sub>S @MoS<sub>2</sub> composite with enhanced photo-Fenton and adsorption  
1074 performance, *Journal of Environmental Chemical Engineering*, 8 (2020) 103762-103762.

1075 [94] Q. Liu, J. Zhao, Y. Wang, Y. Liu, J. Dong, J. Xia, H. Li, The novel photo-Fenton-like few-  
1076 layer MoS<sub>2</sub>/FeVO<sub>4</sub> composite for improved degradation activity under visible light  
1077 irradiation, *Colloids and Surfaces A: Physicochemical and Engineering Aspects*, 623 (2021)  
1078 126721-126721.

1079 [95] W.M. Wang, J. Song, X. Han, Schwertmannite as a new Fenton-like catalyst in the  
1080 oxidation of phenol by H<sub>2</sub>O<sub>2</sub>, *J. Hazard. Mater.*, 262 (2013) 412-419.

1081 [96] H. Duan, Y. Liu, X. Yin, J. Bai, J. Qi, Degradation of nitrobenzene by Fenton-like  
1082 reaction in a H<sub>2</sub>O<sub>2</sub>/schwertmannite system, *Chem. Eng. J.*, 283 (2016) 873-879.

1083 [97] X. Meng, C. Zhang, J. Zhuang, G. Zheng, L. Zhou, Assessment of schwertmannite,  
1084 jarosite and goethite as adsorbents for efficient adsorption of phenanthrene in water and the  
1085 regeneration of spent adsorbents by heterogeneous fenton-like reaction, *Chemosphere*, 244  
1086 (2020) 125523-125523.

1087 [98] N. Nasseh, L. Taghavi, B. Barikbin, M.A. Nasser, A. Allahresani, FeNi<sub>3</sub>/SiO<sub>2</sub> magnetic  
1088 nanocomposite as an efficient and recyclable heterogeneous fenton-like catalyst for the  
1089 oxidation of metronidazole in neutral environments: Adsorption and degradation studies,  
1090 *Composites Part B: Engineering*, 166 (2019) 328-340.

1091 [99] M. Kamranifar, T.J. Al-Musawi, M. Amarzadeh, A. Hosseinzadeh, N. Nasseh, M. Qutob,  
1092 F.S. Arghavan, Quick adsorption followed by lengthy photodegradation using  
1093 FeNi<sub>3</sub>@SiO<sub>2</sub>@ZnO: A promising method for complete removal of penicillin G from  
1094 wastewater, *Journal of Water Process Engineering*, 40 (2021) 101940-101940.

1095 [100] M. Usman, O. Monfort, S. Haderlein, K. Hanna, Enhancement of Pentachlorophenol  
1096 Removal in a Historically Contaminated Soil by Adding Ascorbic Acid to H<sub>2</sub>O<sub>2</sub>/Magnetite  
1097 System, *Catalysts*, 11 (2021) 331.

1098